Search for Third-Generation Scalar Leptoquarks and R-Parity Violating Top Squarks

Kevin Pedro
(University of Maryland)
November 19, 2014

Beyond the Standard Model Physics

- Divergent contributions to the Higgs mass must be canceled (natural) or fine-tuned (unnatural) to achieve the measured value of 125 GeV, instead of Planck scale 10^{19} GeV → hierarchy problem

- Galactic rotation curves and galaxy cluster collisions → dark matter
  Weakly interacting massive particle? (WIMP)

- Grand Unified Theory (GUT) to unite all three fundamental forces
  Expected energy scale of ~10^{16} GeV

- Unification of general relativity and quantum field theory

➢ GUTs (among other BSM theories) predict leptoquarks

➢ Supersymmetry (SUSY) solves hierarchy problem, includes a stable WIMP, and assists in grand unification

Leptoquarks

- Predicted by Grand Unified Theories: Pati-Salam SU(4), Georgi-Glashow SU(5), E_6 superstrings; also technicolor and other compositeness models
- Scalar or vector bosons, carrying: baryon number (B), lepton number (L), color charge, electric charge (Q)
- Intergenerational decays constrained by limits from low-energy processes and flavor-changing neutral current searches
  - Expected to decay to leptons and quarks of the same generation
- Pair production cross sections calculated to NLO in α_s

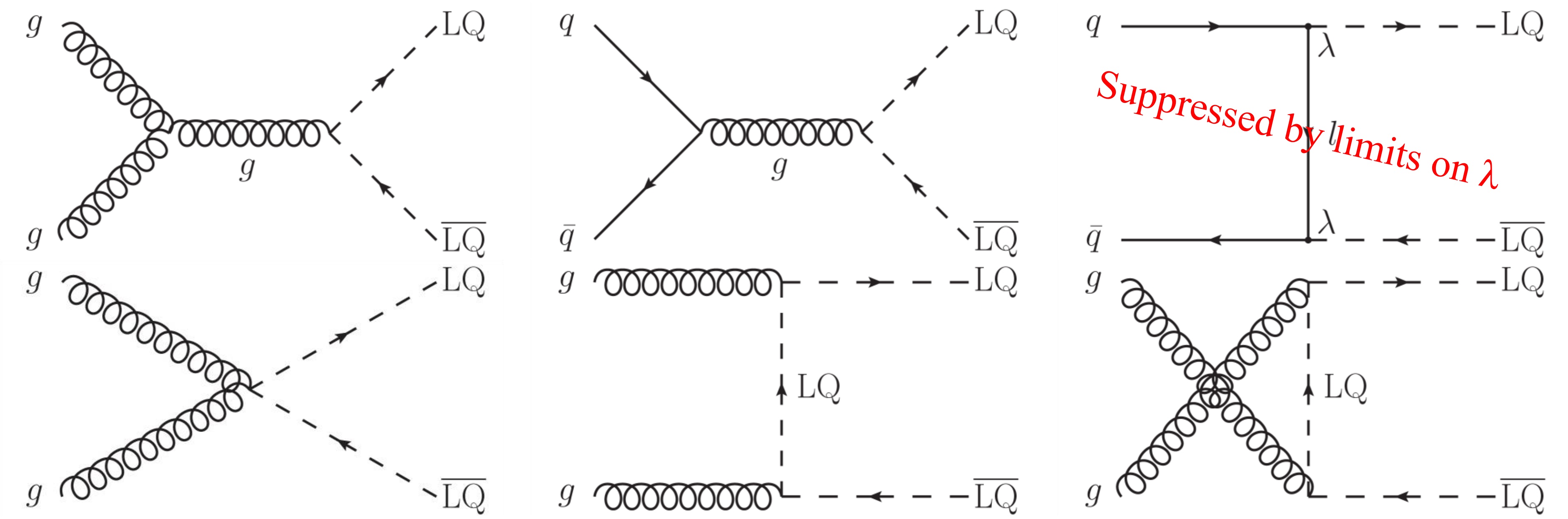

Hierarchy Problem

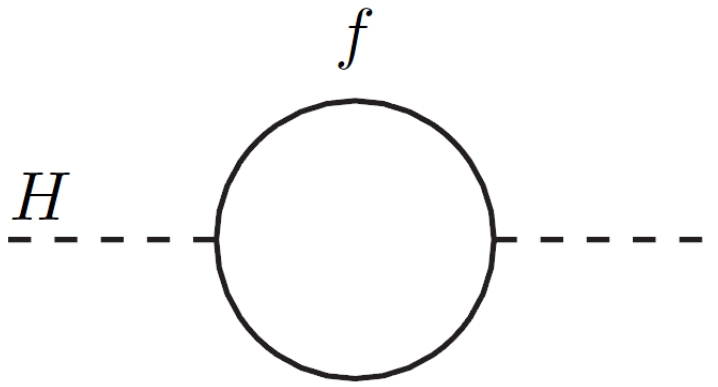

$$\Delta_f m_{\mathrm{H}}^2 = -\frac{|y_f|^2}{8\pi^2}\Lambda_{\mathrm{UV}}^2 + \cdots$$

- Higgs is a scalar particle → no symmetry available to protect its mass value
- Λ_{UV}: cutoff scale to handle the ultraviolet divergence in the loop integral
- Known indications of new physics have $\Lambda_{UV} \sim 10^{16}$ GeV (GUT scale), 10^{19} GeV (Planck scale)
- Even if Λ_{UV} relatively small, contributions from new heavy fermions proportional to y_f, which could be large

Supersymmetry

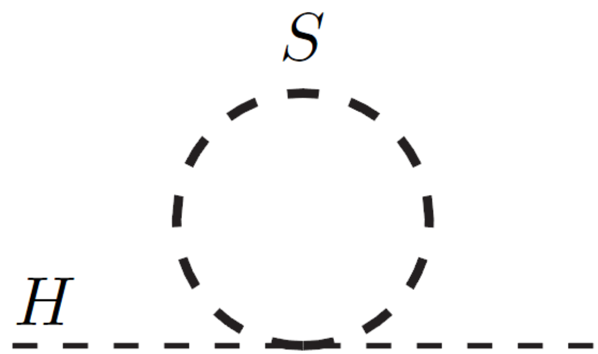

$$\Delta_S m_{\mathrm{H}}^2 = \frac{y_S}{16\pi^2}\Lambda_{\mathrm{UV}}^2 + \cdots$$

- 2 scalar partners (left- and right-handed) for each fermion, with $y_s = |y_f|^2$

➢ Divergent contributions cancel → solves hierarchy problem naturally

- New symmetry: R-parity
  SM particles have $R_p = +1$, SUSY particles have $R_p = -1$
  Lightest SUSY particle (LSP) is stable if R-parity is conserved

$$R = 3B+L+2S = 3(B-L)+2S,\ R_p = (-1)^R$$

Existing Limits on Supersymmetry

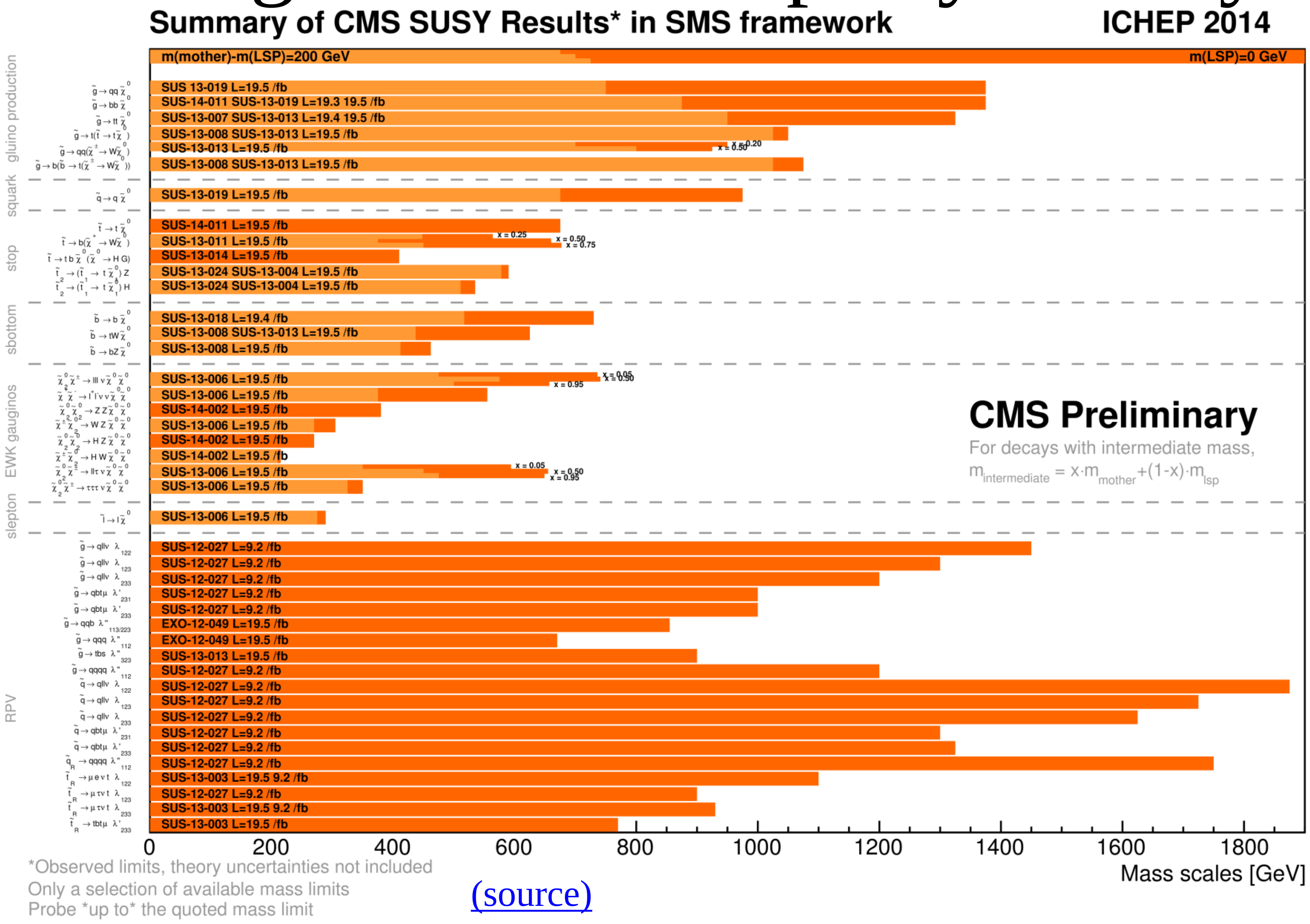

(source)

R-Parity Violation

- R-parity violation allows SUSY particles to decay to final states containing only SM particles
- RPV SUSY still solves the hierarchy problem

$$W_{\mathrm{RPV}} = \frac{1}{2}\lambda_{ijk}L_iL_jE^c_k + \lambda'_{ijk}L_iQ_jD^c_k + \frac{1}{2}\lambda''_{ijk}U^c_iD^c_jD^c_k + \mu_iL_iH_u$$

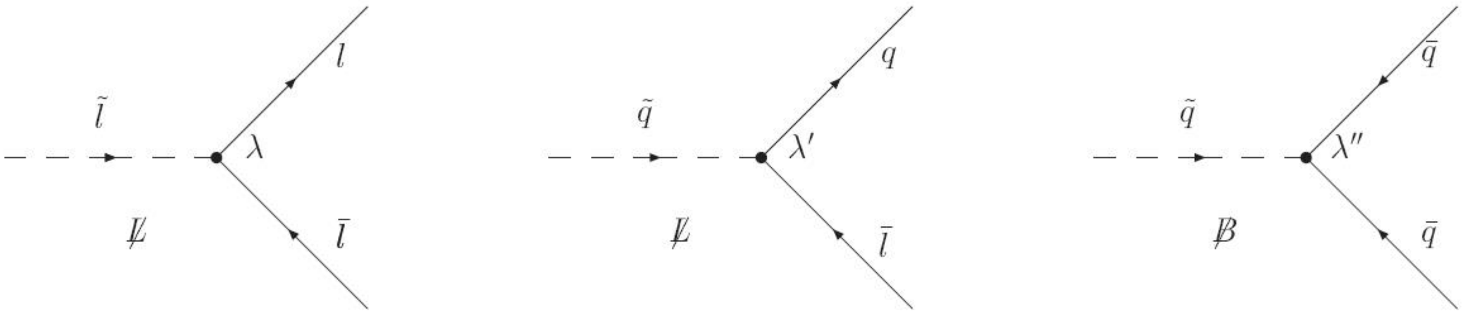

- Decays present signatures without high missing transverse energy, avoiding limits on much of the parameter space of R-parity conserving SUSY
- Top squarks and higgsinos are typically lighter than the other scalar SUSY particles in natural models

➢ Third generation of superpartners potentially accessible at LHC energies

- Searches consider simplified models with other SUSY particles decoupled

Searches

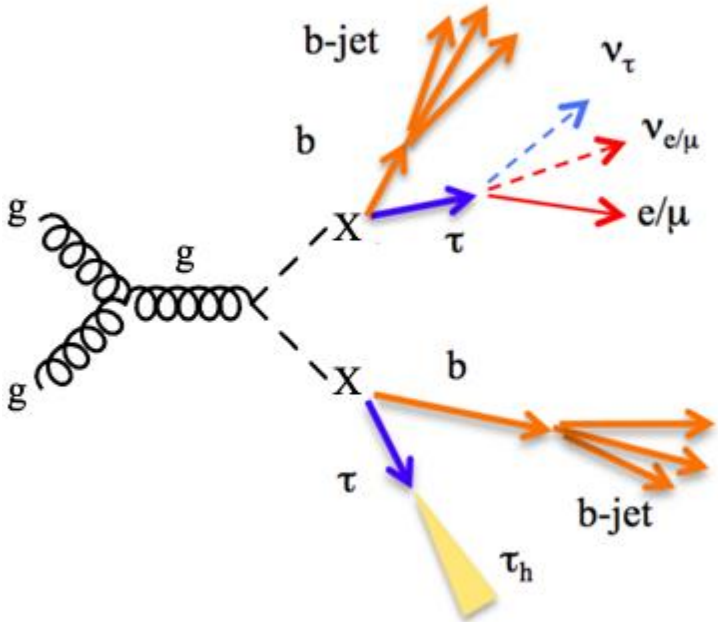

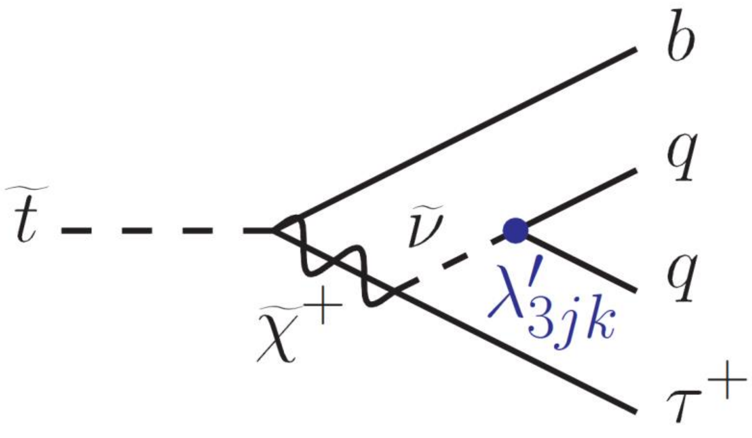

<u>Leptoquark search</u>

LQ → τb

$\tilde{t} \to \tau b$ via λ'_{333} coupling

Same kinematic distributions and final state (two channels):

$e\tau_h bb$, $\mu\tau_h bb$

<u>Top squark search</u>

$\tilde{t} \to \tilde{\chi}^\pm b$, $\tilde{\chi}^\pm \to \tilde{\nu}\tau \to qq\tau$

$M_{\tilde{t}} - M_{\tilde{\chi}^\pm} = 100$ GeV $< M_t$

$\tilde{\nu}$ decay via λ'_{3jk} (j, k = 1, 2)

Similar final state:

$e\tau_h bb4j$, $\mu\tau_h bb4j$

- LQ and $\tilde{t}$ have the same pair production cross section in decoupled models

The CMS Detector

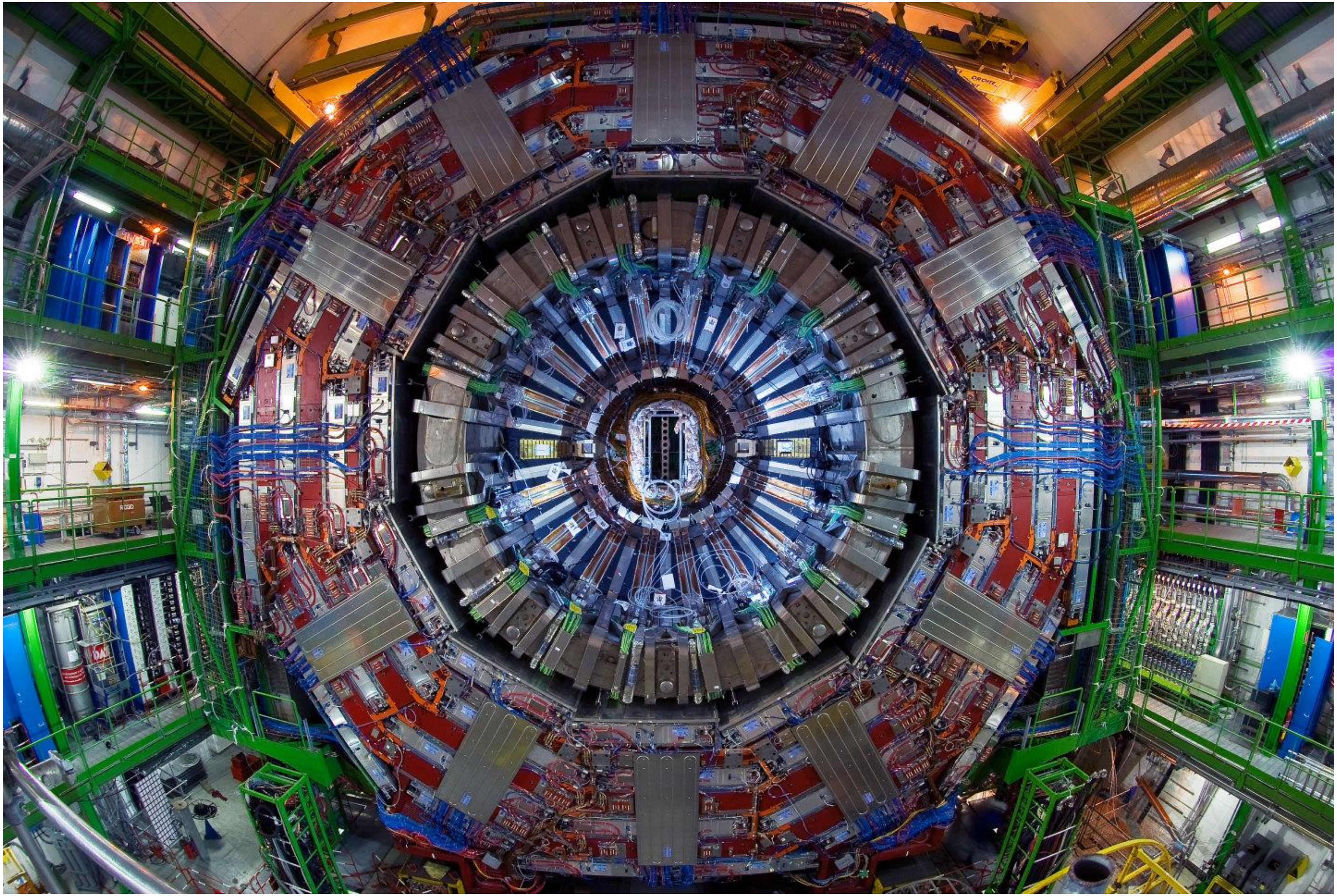

(source)

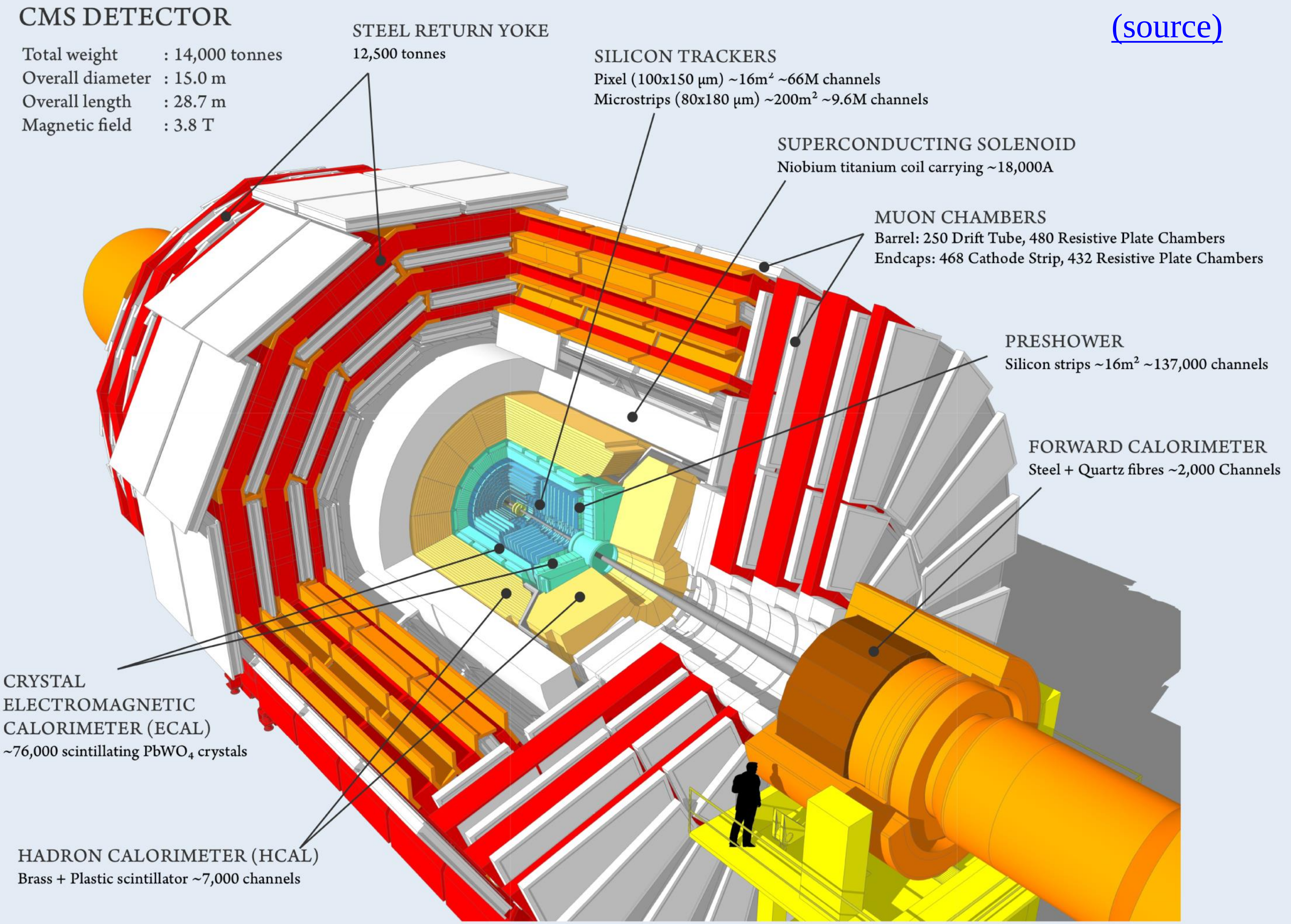
CMS DETECTOR
Total weight : 14,000 tonnes
Overall diameter : 15.0 m
Overall length : 28.7 m
Magnetic field : 3.8 T
STEEL RETURN YOKE
12,500 tonnes
SILICON TRACKERS
Pixel (100x150 μm) ~16m² ~66M channels
Microstrips (80x180 μm) ~200m² ~9.6M channels
SUPERCONDUCTING SOLENOID
Niobium titanium coil carrying ~18,000A
MUON CHAMBERS
Barrel: 250 Drift Tube, 480 Resistive Plate Chambers
Endcaps: 468 Cathode Strip, 432 Resistive Plate Chambers
PRESHOWER
Silicon strips ~16m² ~137,000 channels
FORWARD CALORIMETER
Steel + Quartz fibres ~2,000 Channels
CRYSTAL ELECTROMAGNETIC CALORIMETER (ECAL)
~76,000 scintillating PbWO4 crystals
HADRON CALORIMETER (HCAL)
Brass + Plastic scintillator ~7,000 channels

CMS 2012 Luminosity

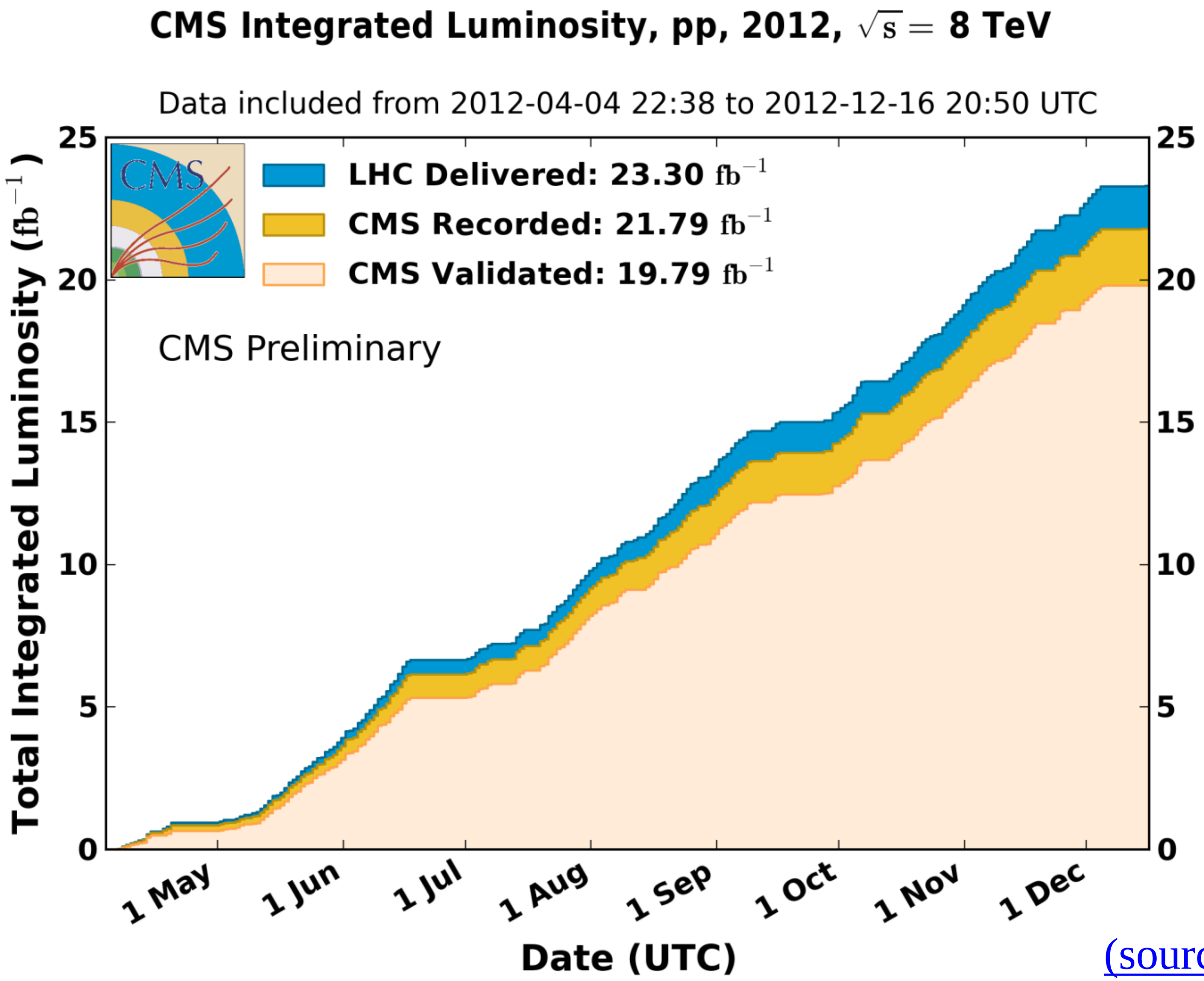

(source)

- Measured by counting clusters in the pixel, systematic uncertainty only 2.6%

Particle Flow

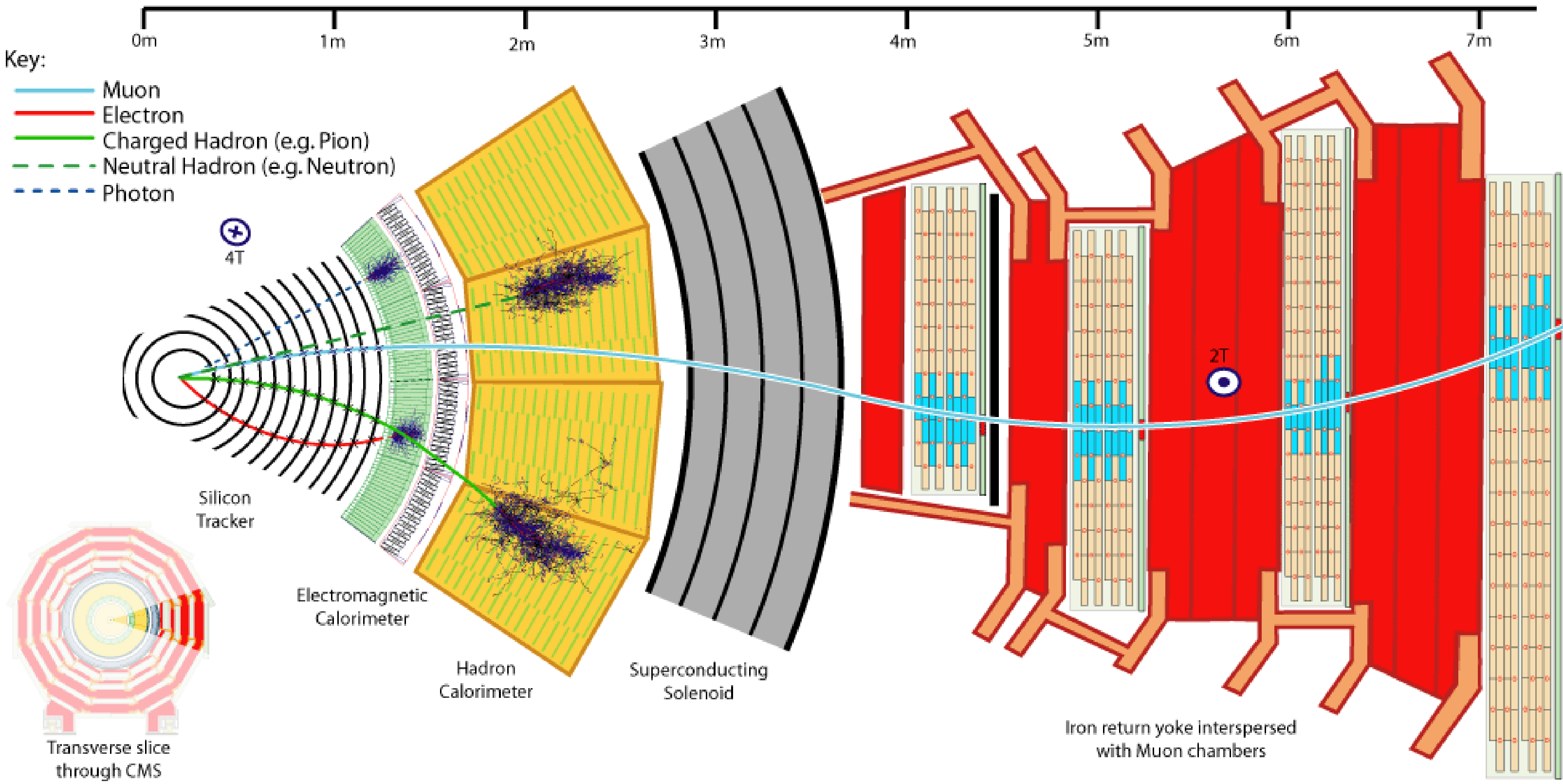

Tracker hits → charged tracks
ECAL hits → clusters
HCAL hits → clusters
Muon hits → muon tracks

} linking → Blocks: electrons, muons, photons, charged hadrons, neutral hadrons

Hadron Plus Strips Algorithm

- 64.76% of tau leptons will decay to hadrons

Decay	Resonance	Mass (MeV/c^2)	Branching fraction (%)
$\tau^- \to h^- \nu_\tau$			11.53%
$\tau^- \to h^- \pi^0 \nu_\tau$	ρ^-	775	25.95%
$\tau^- \to h^- \pi^0 \pi^0 \nu_\tau$	a_1^-	1230	9.52%
$\tau^- \to h^- h^+ h^- \nu_\tau$	a_1^-	1230	9.80%
$\tau^- \to h^- h^+ h^- \pi^0 \nu_\tau$			4.76%

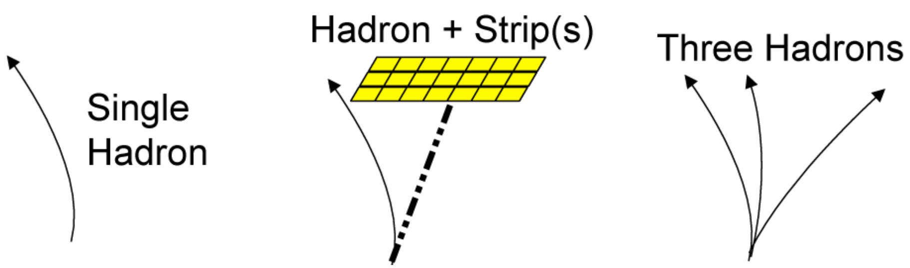

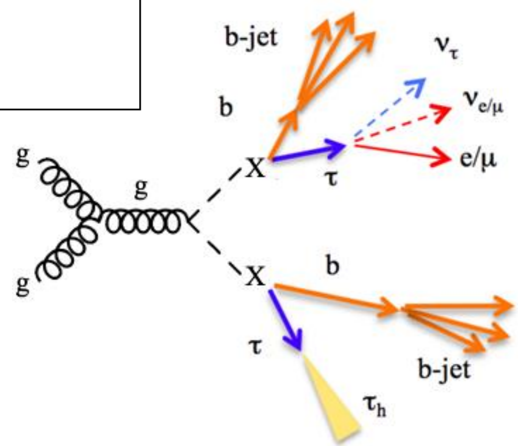

- CMS uses the **Hadron Plus Strips** (HPS) algorithm to reconstruct τ_h decays
  1. Start from a Particle Flow jet
  2. Reconstruct photons from π^0 decays as electromagnetic strips, to account for conversions in the tracker
  3. Combine identified strips (if any) with charged hadrons
  4. Reconstruct four-momenta from the constituent particles according to decay and mass hypotheses

Tau Performance

- Electron-tau discriminator: multivariate, considers association of τ_h with GSF tracks and electron candidates
- Muon-tau discriminator: cut-based, minimize muon system activity around τ_h and reject minimum ionizing signatures
- Jet-tau discriminator: Particle Flow isolation, τ_hs tend to be narrower than jets

$$I^{\mathrm{PF}}_{\tau_{\mathrm{h}}} = \sum_{\Delta R<0.5} p_{\mathrm{T}}^{(\mathrm{CH})} + \max\left(\sum_{\Delta R<0.5} p_{\mathrm{T}}^{(\gamma)} - \Delta\beta \sum_{\Delta R<0.8} p_{\mathrm{T}}^{(\mathrm{PU})}, 0\right)$$

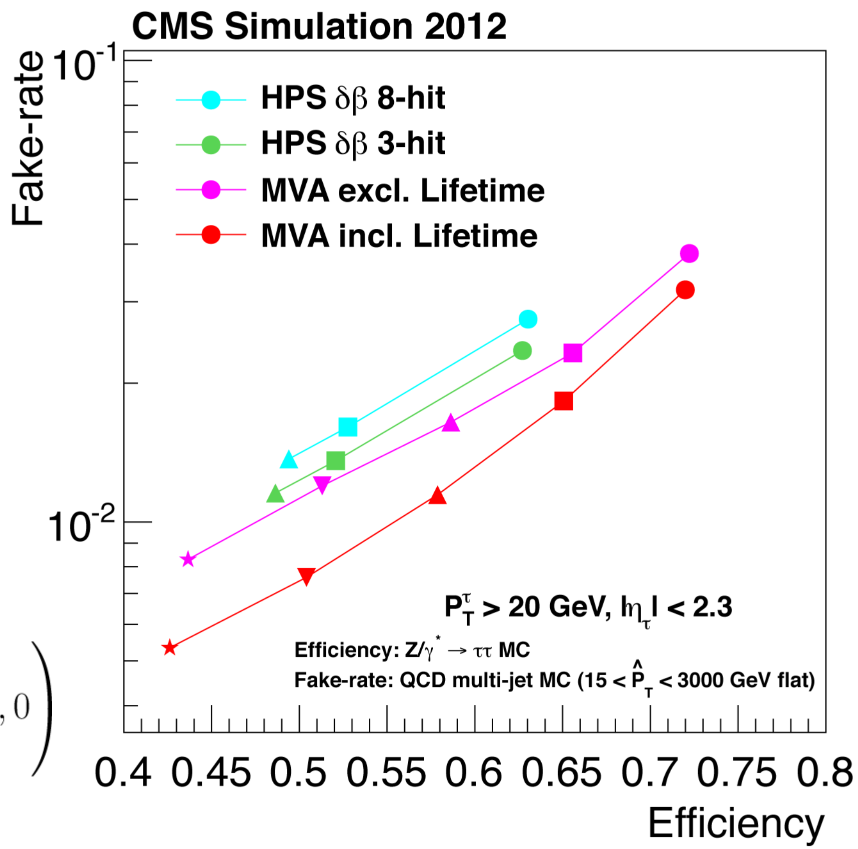

Data-MC agreement: ~6% in efficiency, ~20% in fake rate

Reference: “Tau ID Performance Plots”, CMS-DP-2014-015

Object Identification

Muon

$p_T > 30$ GeV, $|\eta| < 2.1$
Identified with Particle Flow
(tracker + muon system)

Electron

$p_T > 30$ GeV, $|\eta|$ in ECAL
Identified w/ Gaussian Sum Filter
(tracker + ECAL)

Tau

$p_T > 30$ GeV, $|\eta| < 2.3$
Identified with Particle Flow
(tracker + calorimeters)

Jets

$p_T > 30$ GeV, $|\eta| < 2.4$
Identified with Particle Flow
b-tagging: CSV loose

High Level Trigger

HLT_IsoMu24
HLT_Ele27_WP80

Corrections

Pileup reweighting
Lepton data/MC efficiency
b-tag & mistag scale factors

Selection

Preselection

- One identified and isolated e (μ)
- One identified and isolated τ_h
- $dR(\ell,\tau_h) > 0.5$,
  $vertex(\ell) = vertex(\tau_h)$,
  $charge(\ell) \neq charge(\tau_h)$
- Veto opposite sign μ (e)
- Veto opposite sign loose e (μ)
  [loose ID/iso, $p_T > 20$ GeV]
- $N_{jets} \geq 2$
- $dR(j,\ell) > 0.5$, $dR(j,\tau_h) > 0.5$

Main Selection

- $N_{b\text{-}jet} \geq 1$
- $p_T(\tau_h) > 50$ GeV

LQ Final Selection

- $M(\tau_h,jet) > 250$ GeV

$\tilde{t}$ Final Selection

- $N_{jets} \geq 5$

Key Variables

- $M(\tau_h,\text{jet})$: invariant mass of the τ_h paired with a selected jet
  Pairing is chosen that minimizes $|M(\tau_h,\text{jet } i) - M(\ell,\text{jet } j)|$

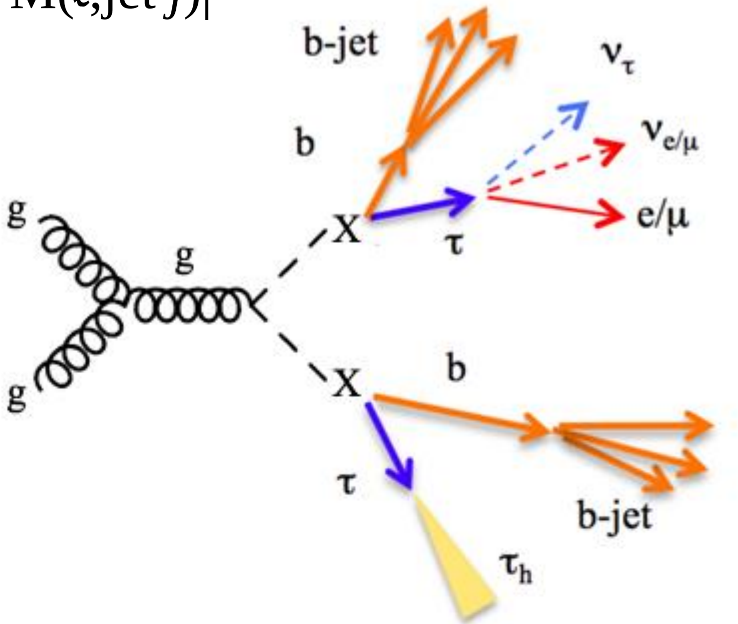

- S_T: scalar sum of p_T of all final state objects
  Distribution is used to set CL_s limits

$$S_{\mathrm{T}}^{(\mathrm{LQ})} = p_{\mathrm{T}}(\ell) + p_{\mathrm{T}}(\tau) + p_{\mathrm{T}}(\text{b-jet}) + p_{\mathrm{T}}(\text{jet})$$

$$S_{\mathrm{T}}^{(\widetilde{\mathrm{t}})} = p_{\mathrm{T}}(\ell) + p_{\mathrm{T}}(\tau) + p_{\mathrm{T}}(\text{b-jet}) + \sum_{i=1}^{4} p_{\mathrm{T}}(\text{jet } i)$$

Leptoquark Candidate Event

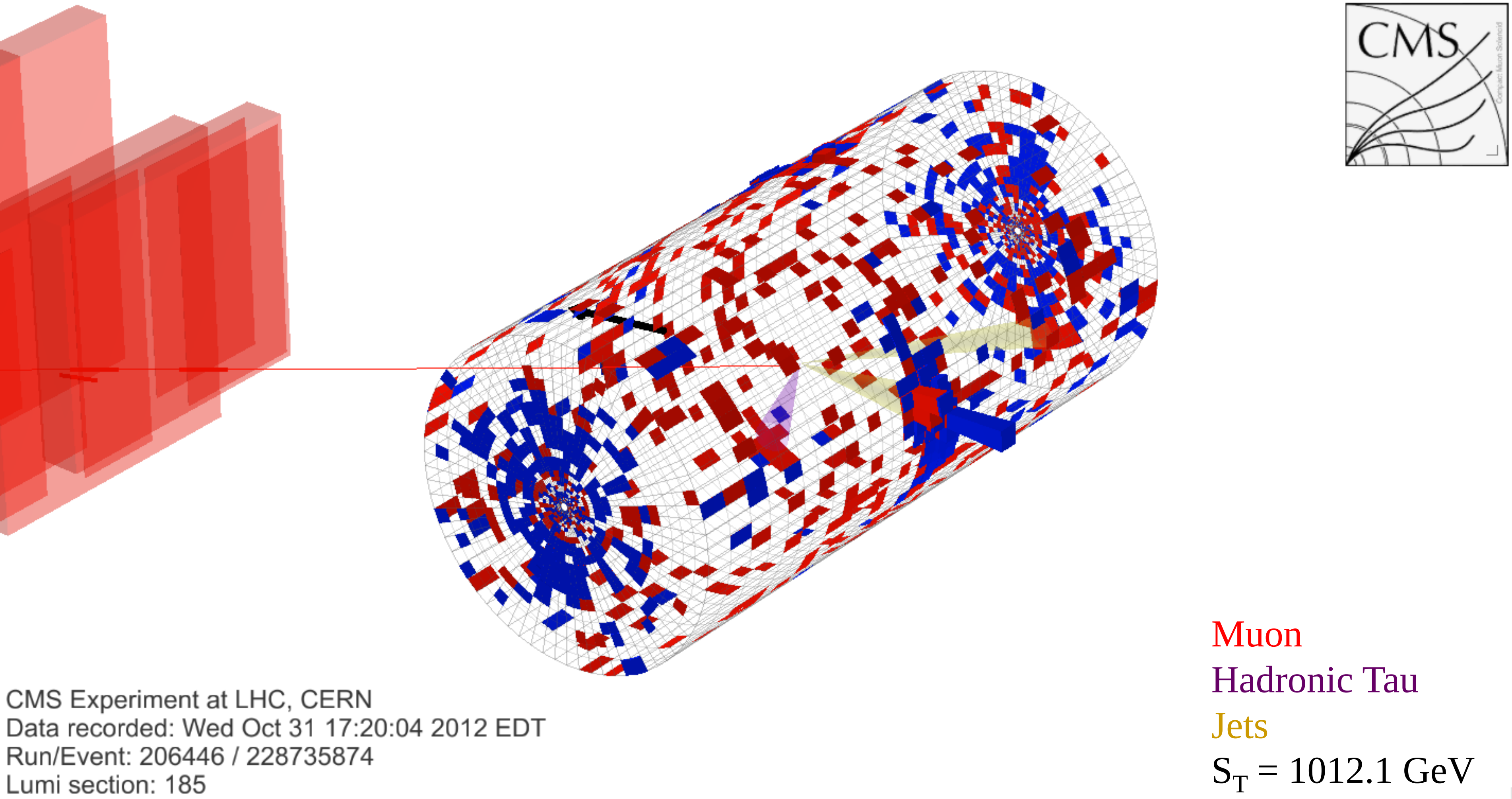

Muon
Hadronic Tau
Jets
S_T = 1012.1 GeV

Top Squark Candidate Event

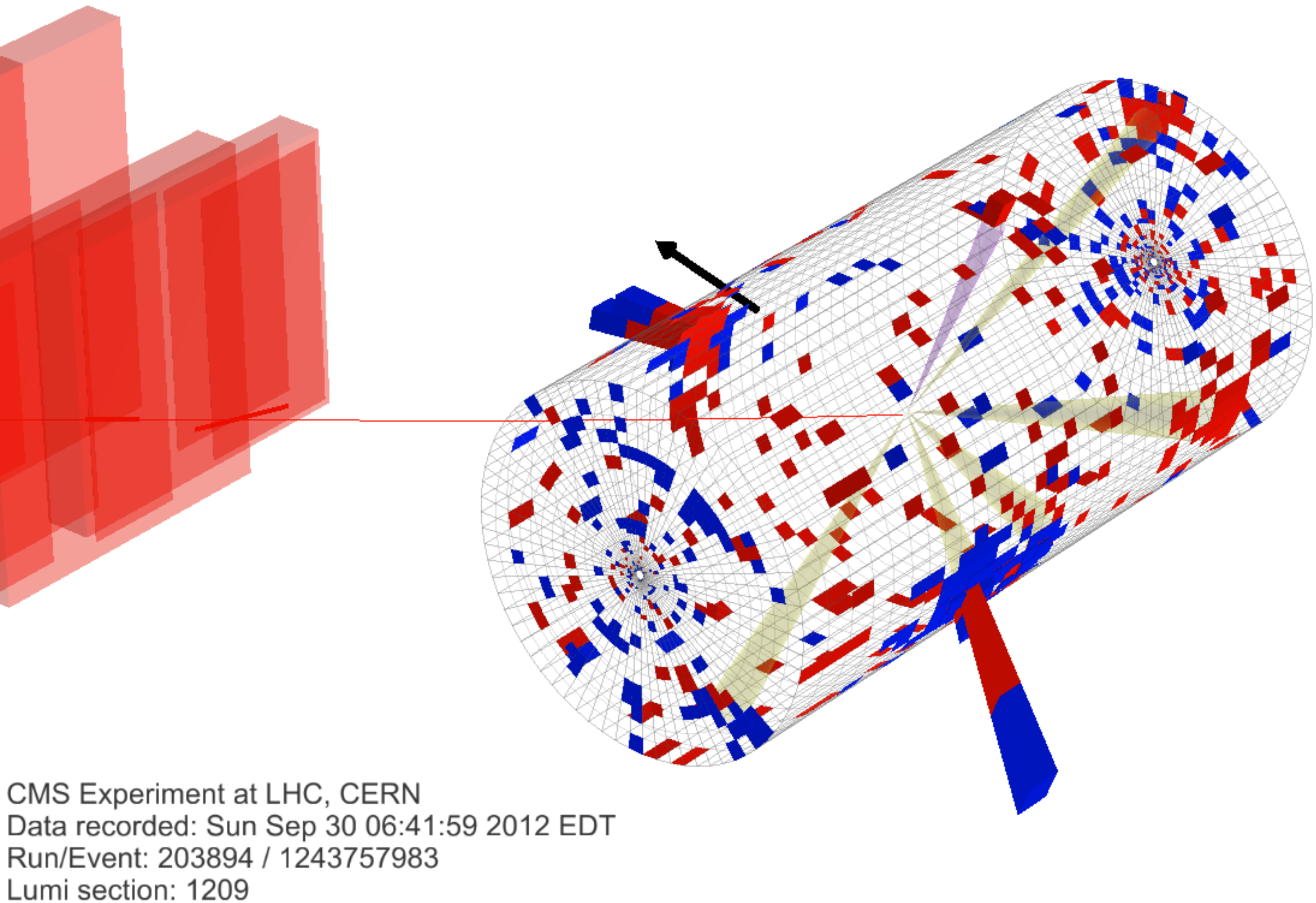

Muon
Hadronic Tau
Jets
S_T = 1586.2 GeV

Major Backgrounds

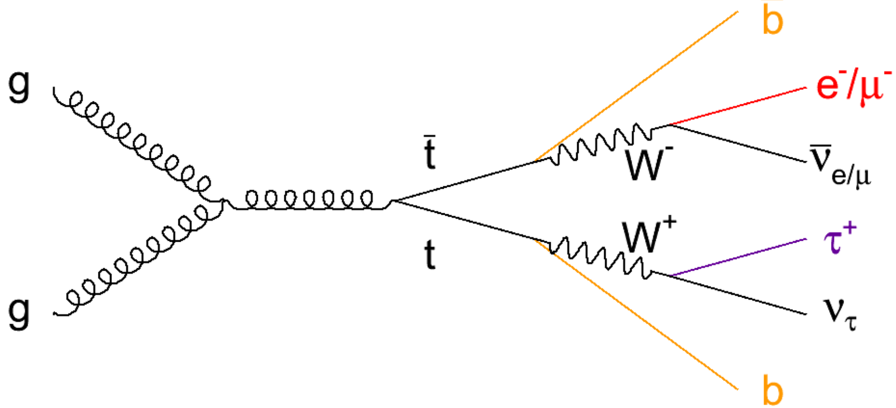

Major irreducible background:
$t\bar{t}$ with genuine τ_h (purple)

Major reducible background from jets misidentified as τ_h:
$t\bar{t}$, W + jets, Z + jets, QCD multijets

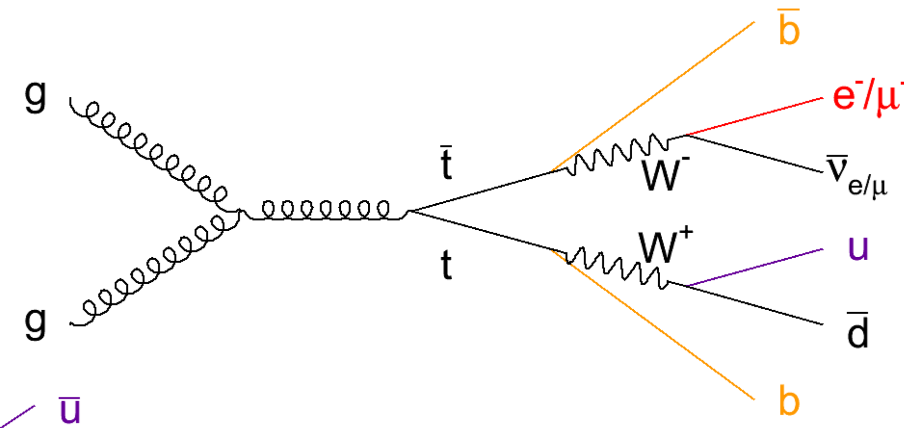

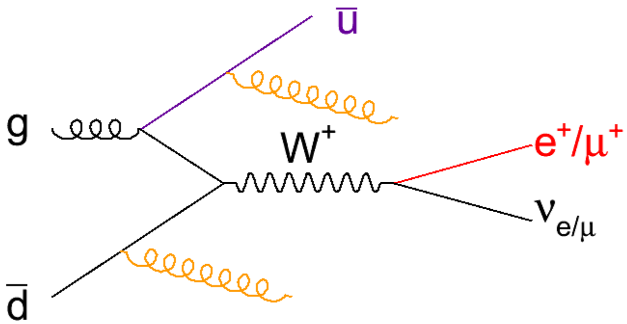

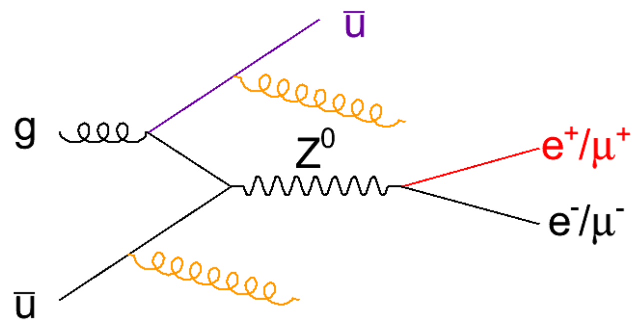

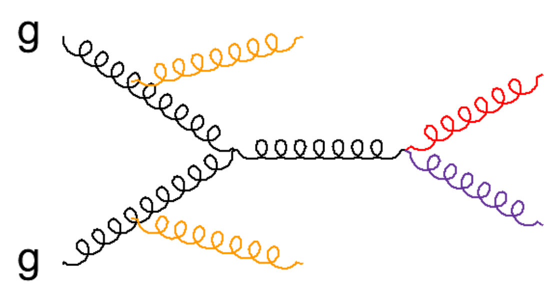

Minor Backgrounds

Minor backgrounds:

$Z \to \tau^+\tau^-$ + jets, single top, diboson

and processes where a lepton is misidentified as a τ_h ($t\bar{t}$, Z + jets)

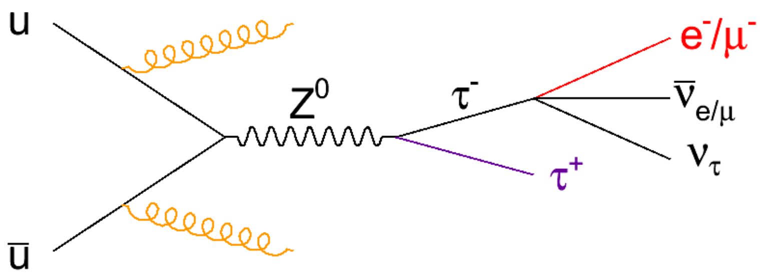

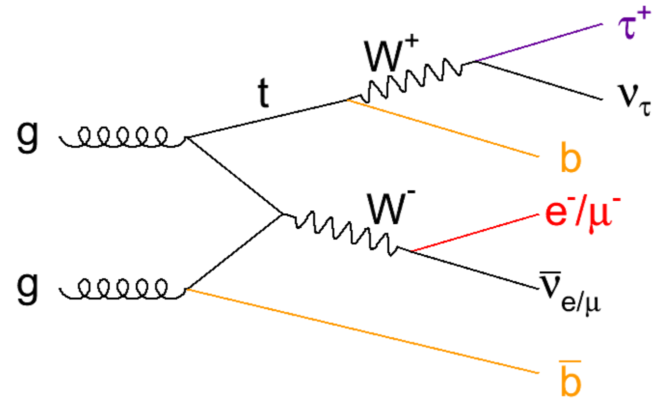

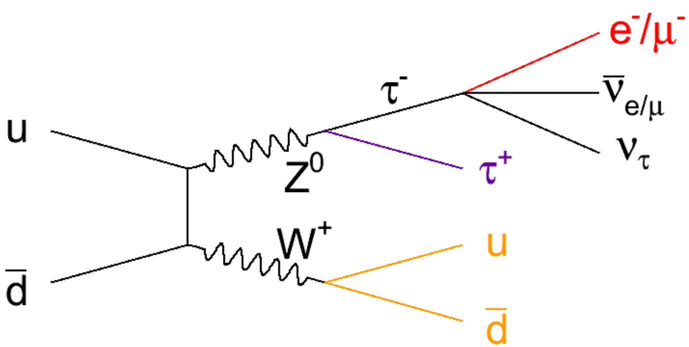

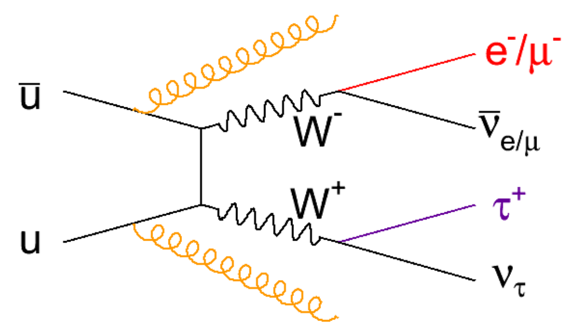

Background Estimations

- Major backgrounds estimated using observed data
- Minor backgrounds estimated using MC simulation

MC simulation details:

- *PYTHIA6*: leptoquark, top squark, diboson
- *MADGRAPH*: $t\bar{t}$, W + jets, Z + jets
- *POWHEG*: single top
- *TAUOLA* is used for processes containing genuine tau leptons

Irreducible $t\bar{t}$ Bkg. Estimation

The eμ control region can be used to estimate the irreducible $t\bar{t}$ background (containing genuine taus) from data for the $\ell\tau$ channels.

eμ channel

$t\bar{t}$ simulation (w/ scale factors)

Madgraph, PDG

$$N_{\ell\tau_h} = N_{e\mu} \times \frac{\varepsilon^{\mathrm{sel}}_{\ell\tau_h}\rho^{\mathrm{sel}}_{\ell\tau_h}}{\varepsilon^{\mathrm{sel}}_{e\mu}\rho^{\mathrm{sel}}_{e\mu}} \times \frac{\varepsilon^{\mathrm{ID}}_{\ell}\varepsilon^{\mathrm{ID}}_{\tau_h}}{\varepsilon^{\mathrm{ID}}_{e}\varepsilon^{\mathrm{ID}}_{\mu}} \times \frac{\mathcal{A}_{\ell\tau_h}B_{W\ell}B_{W\tau_h} + \mathcal{A}_{\tau_\ell\tau_h}B_{W\tau_\ell}B_{W\tau_h}}{\mathcal{A}_{e\mu}B_{We}B_{W\mu} + \mathcal{A}_{\mu\tau_e}B_{W\mu}B_{W\tau_e} + \mathcal{A}_{e\tau_\mu}B_{We}B_{W\tau_\mu} + \mathcal{A}_{\tau_e\tau_\mu}B_{W\tau_e}B_{W\tau_\mu}}$$

The yield from the eμ channel is multiplied by a combination of selection efficiencies, data/MC scale factors, identification efficiencies, acceptances, and branching ratios. This relates the eμ channel to the $\ell\tau$ channels for ℓ = e, μ.

Systematic uncertainties are assigned based on statistical uncertainty in the eμ control region and the propagation of uncertainties in the acceptances and efficiencies. The total systematic uncertainty on the yield is 19–22%, depending on the channel and the search.

eμ Control Region Plots (1)

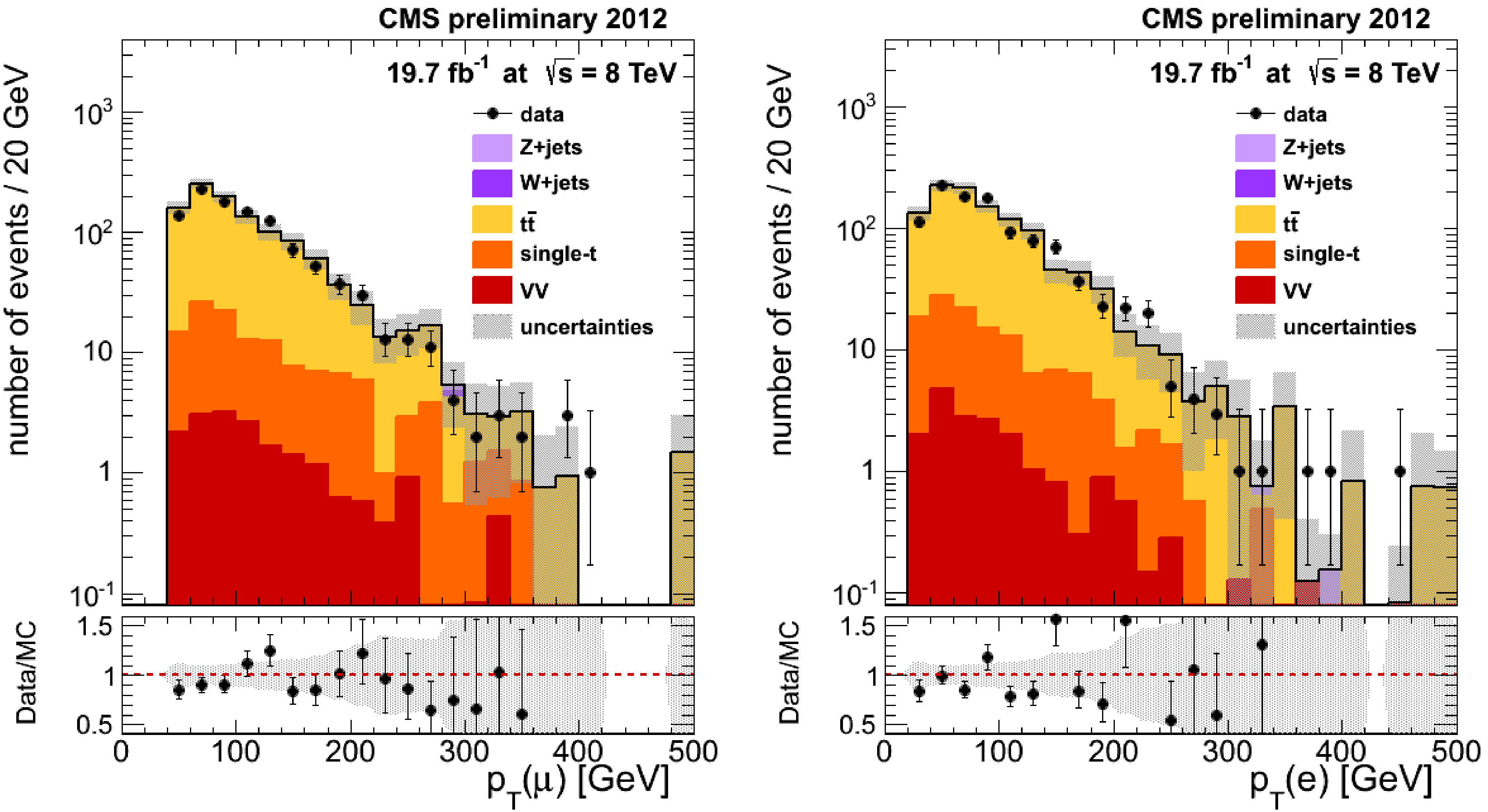

Excellent agreement between data and MC in the eμ channel, after the LQ final selection.

eμ Control Region Plots (2)

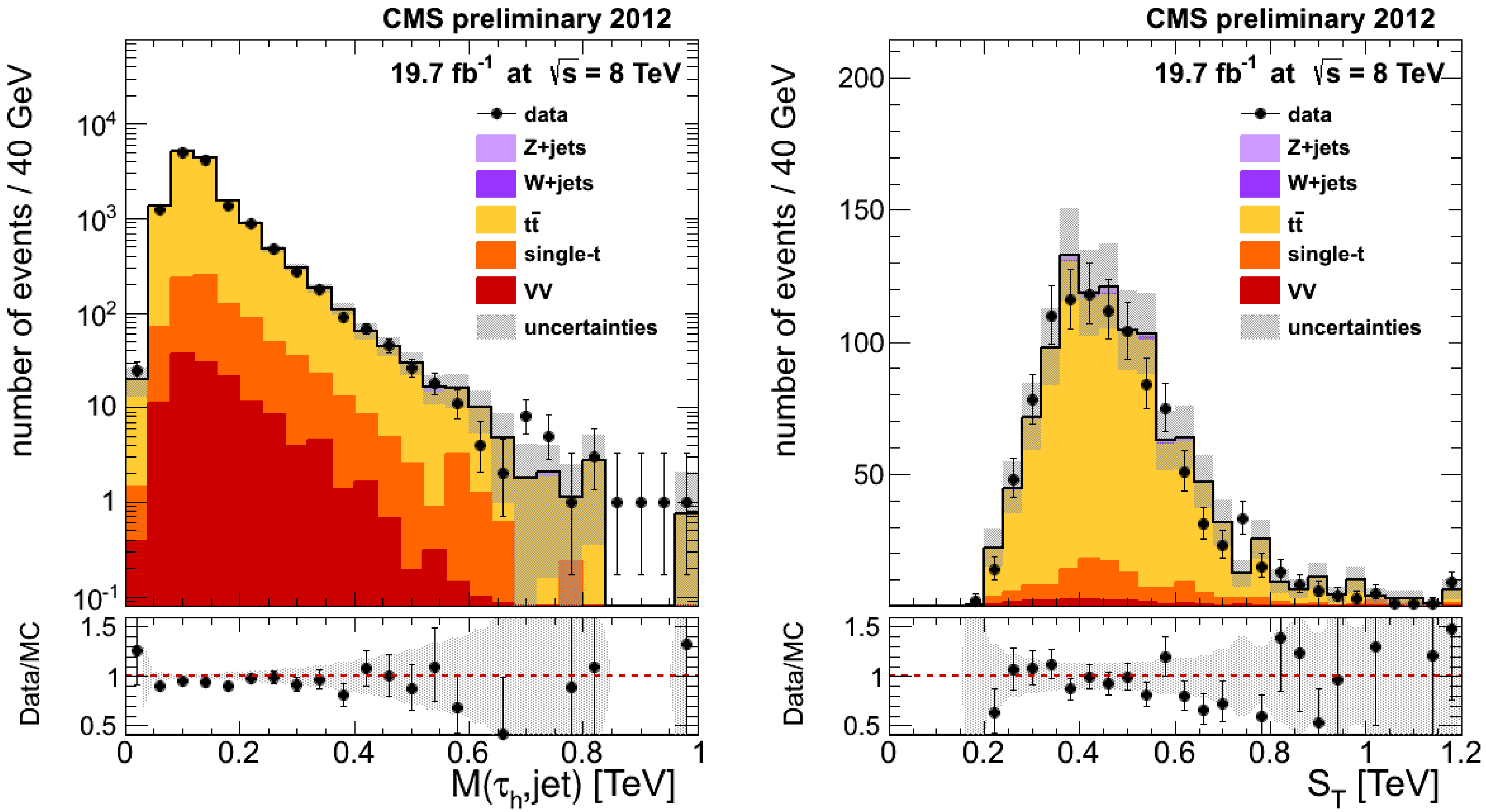

Excellent agreement between data and MC in the eμ channel, after the LQ final selection.

Major Reducible Bkg. Estimation

The major reducible background from the misidentification of jets as taus ("fake tau" background) can be estimated from data using two control regions: $Z \rightarrow \mu\mu$+jets and anti-isolated taus.

$$f(p_{\mathrm{T}}) = \frac{N_{\mathrm{iso}\ \tau}^{(\mathrm{Z}\rightarrow\mu\mu)}(p_{\mathrm{T}})}{N_{\mathrm{all}\ \tau}^{(\mathrm{Z}\rightarrow\mu\mu)}(p_{\mathrm{T}})}$$

→ from $Z \rightarrow \mu\mu$+jets control region

$$N_{\mathrm{misID}\ \tau} = \sum_{\mathrm{events}}^{(\mathrm{anti\text{-}iso})} \frac{1 - \prod_{\tau}\left[1 - f\left(p_{\mathrm{T}}(\tau)\right)\right]}{\prod_{\tau}\left[1 - f\left(p_{\mathrm{T}}(\tau)\right)\right]}$$

→ from anti-isolated control region (in each $\ell\tau$ channel)

Systematic uncertainty is derived from varying the misidentification probability (based on statistical uncertainty, N_{jets} requirement, and type of process) and the residual MC in the anti-iso region. Statistical uncertainty from the anti-iso region is negligible. The total systematic uncertainty on the yield is 16–24%, depending on the channel and the search.

$Z \rightarrow \mu\mu$ Control Region Plots

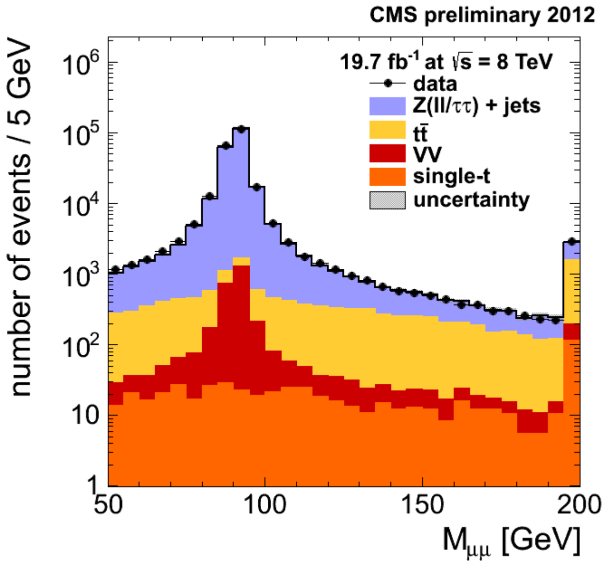

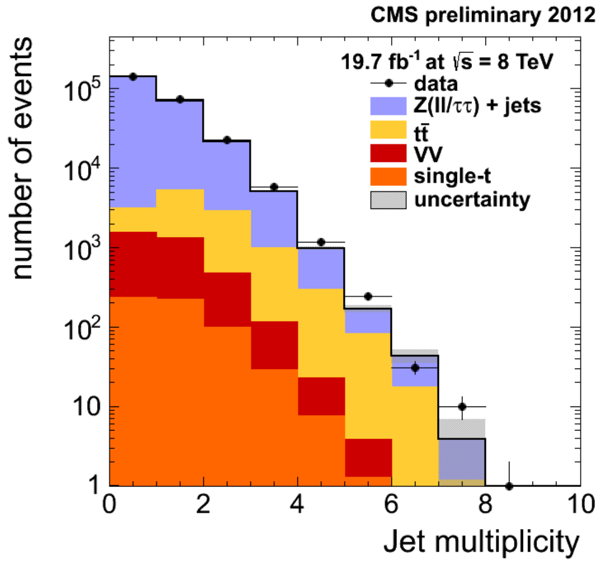

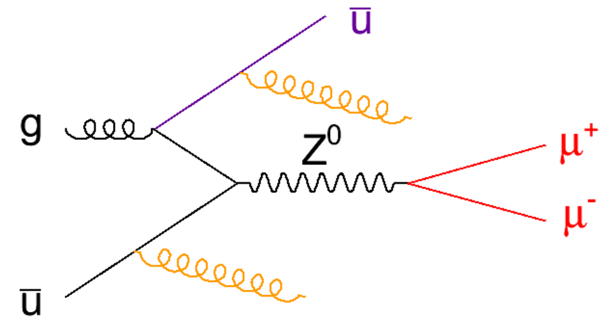

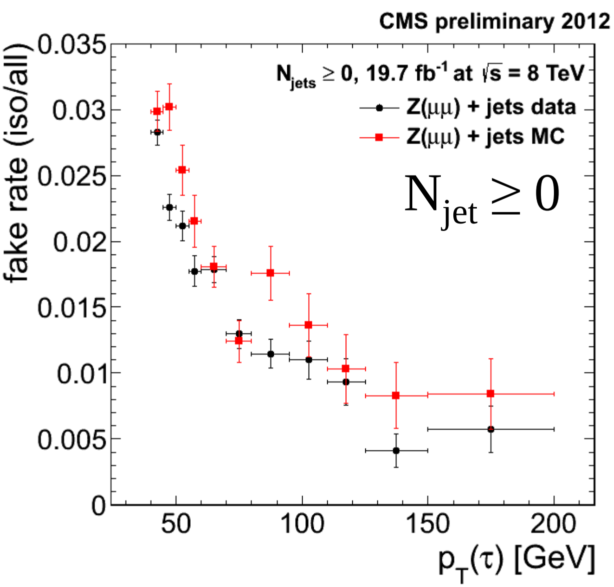

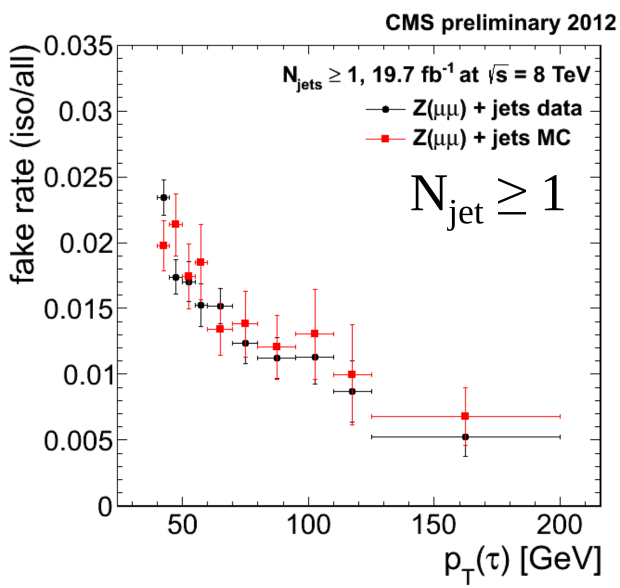

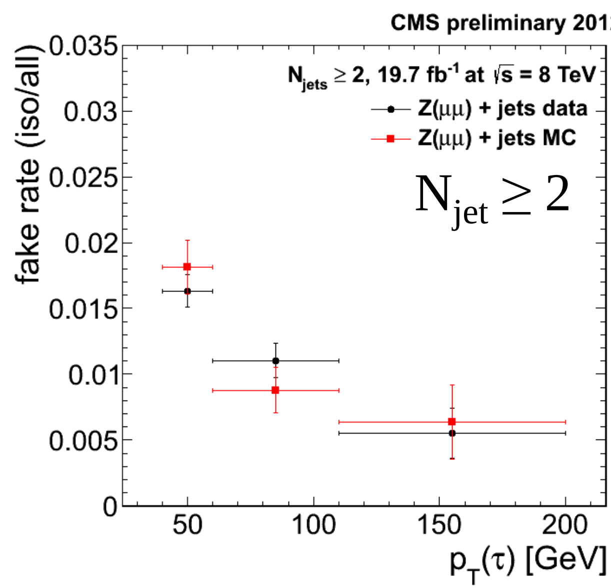

Anti-iso Control Region Plots (LQ)

μτ channel

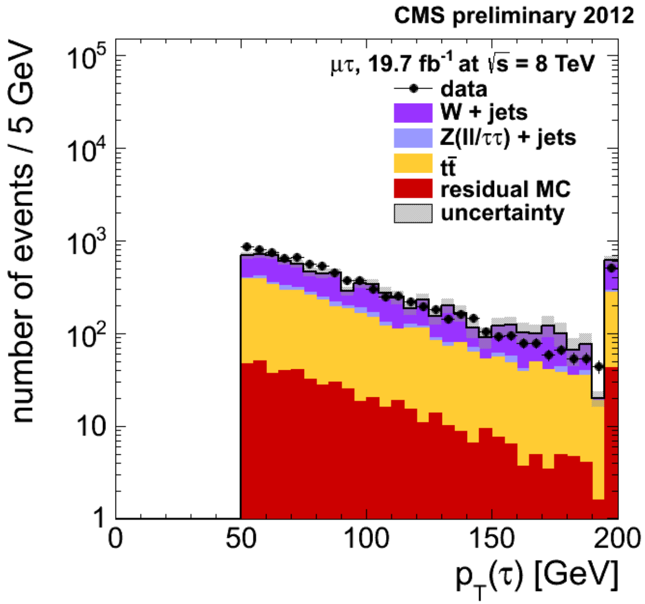

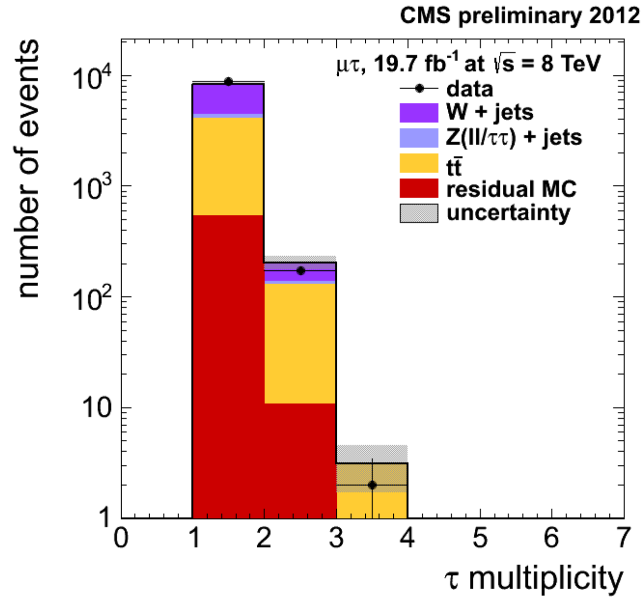

eτ channel

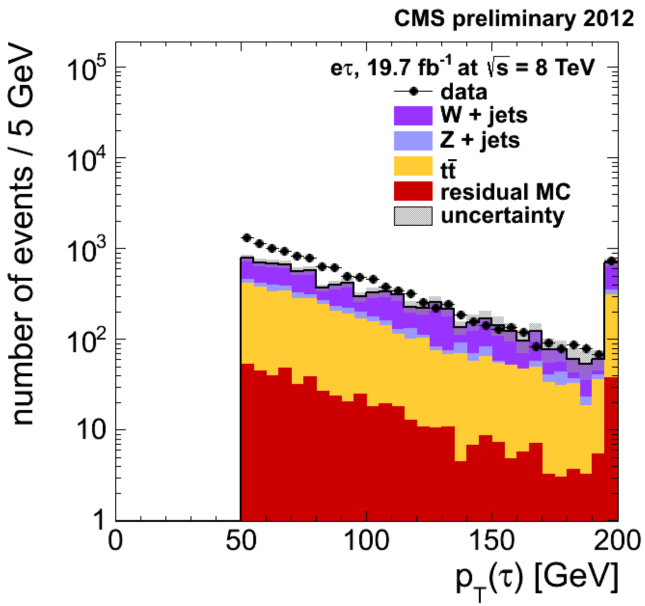

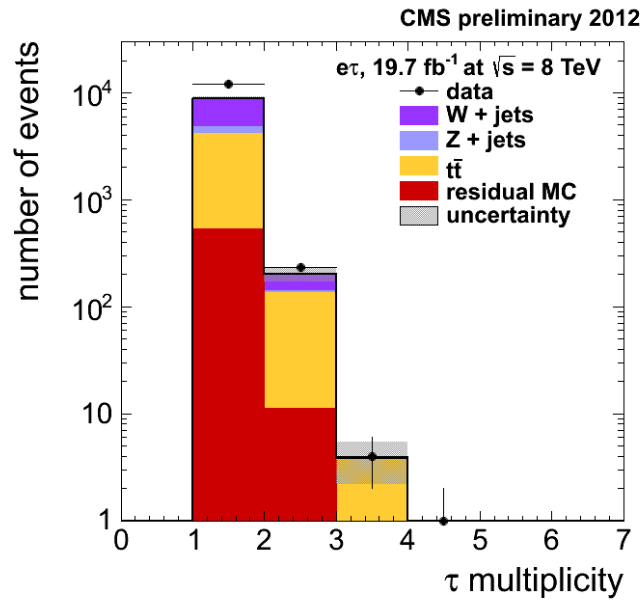

Anti-iso Control Region Plots ($\tilde{t}$)

μτ channel

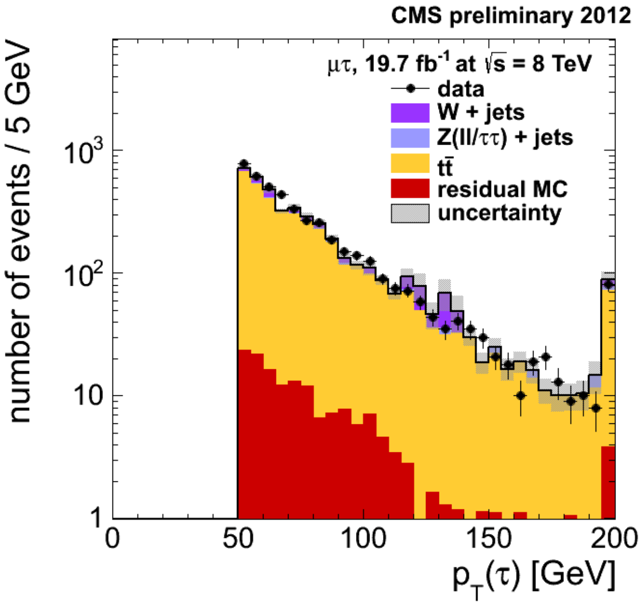

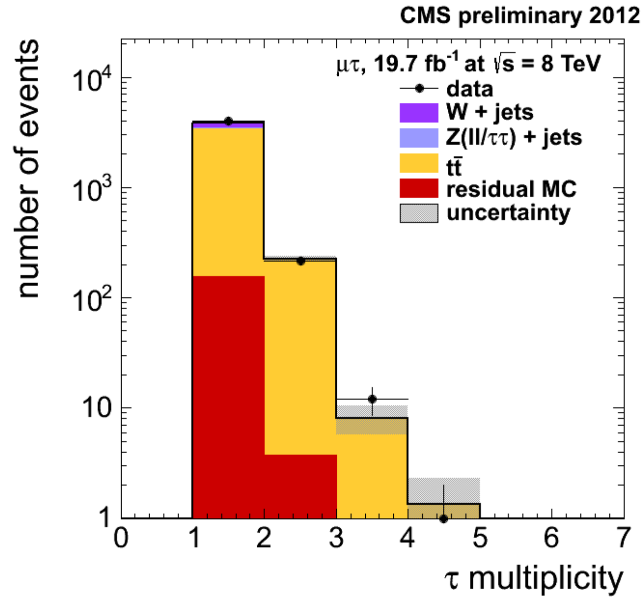

eτ channel

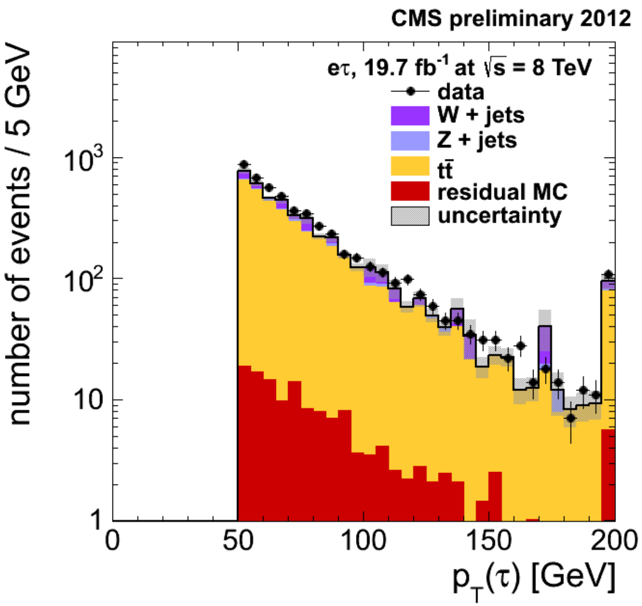

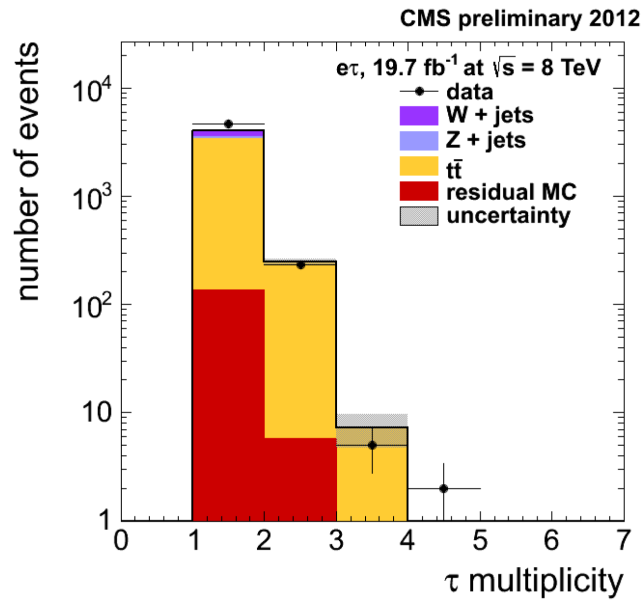

QCD Multijets Bkg. Estimation (1)

MisID probability from V+jets events: mostly quark jets
QCD: mostly gluon jets, so V+jets misID probability is not appropriate

(This background only contributes to the $e\tau_h$ channel in the LQ search)

1. Same sign/opposite sign (SS/OS) method to estimate # of QCD events:

$$N_{\text{QCD}}^{\text{OS}} = 1.06\left(N_{\text{data}}^{\text{SS}} - N_{\text{MC}}^{\text{SS}}\right)$$

2. Subtract contribution from QCD in anti-iso control region: 38.5 ± 2.7 events

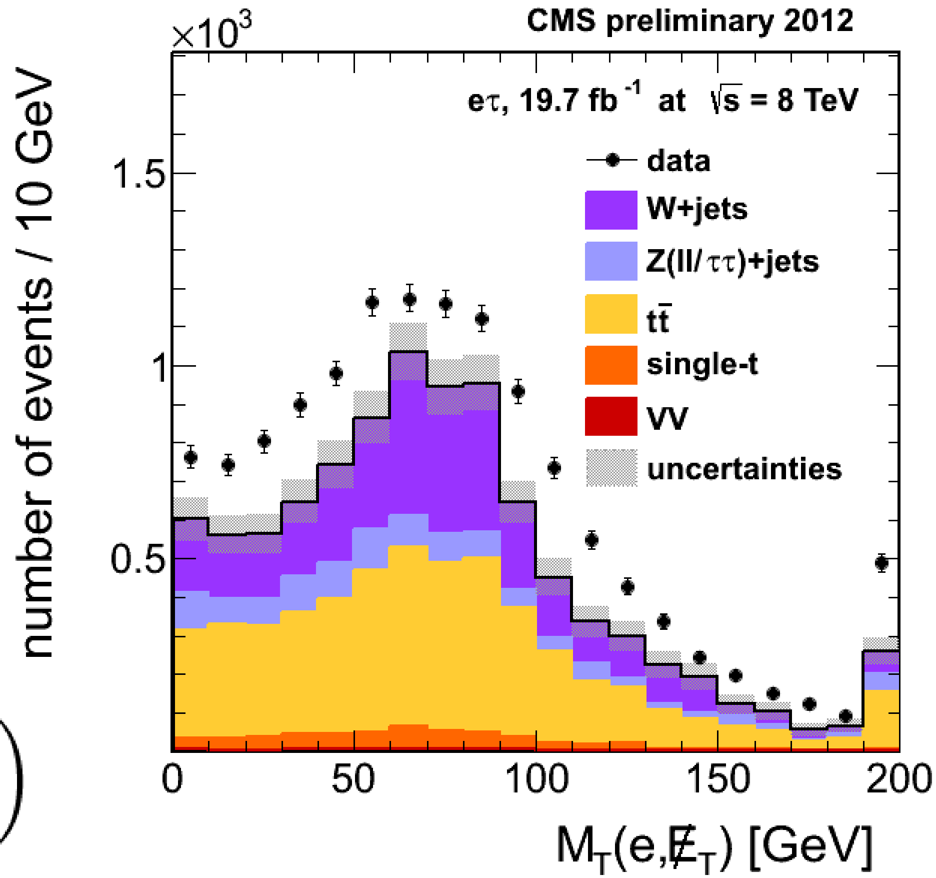

Transverse mass in the same-sign anti-iso region (used for QCD subtraction). The overall excess in data indicates the presence of QCD.

QCD Multijets Bkg. Estimation (2)

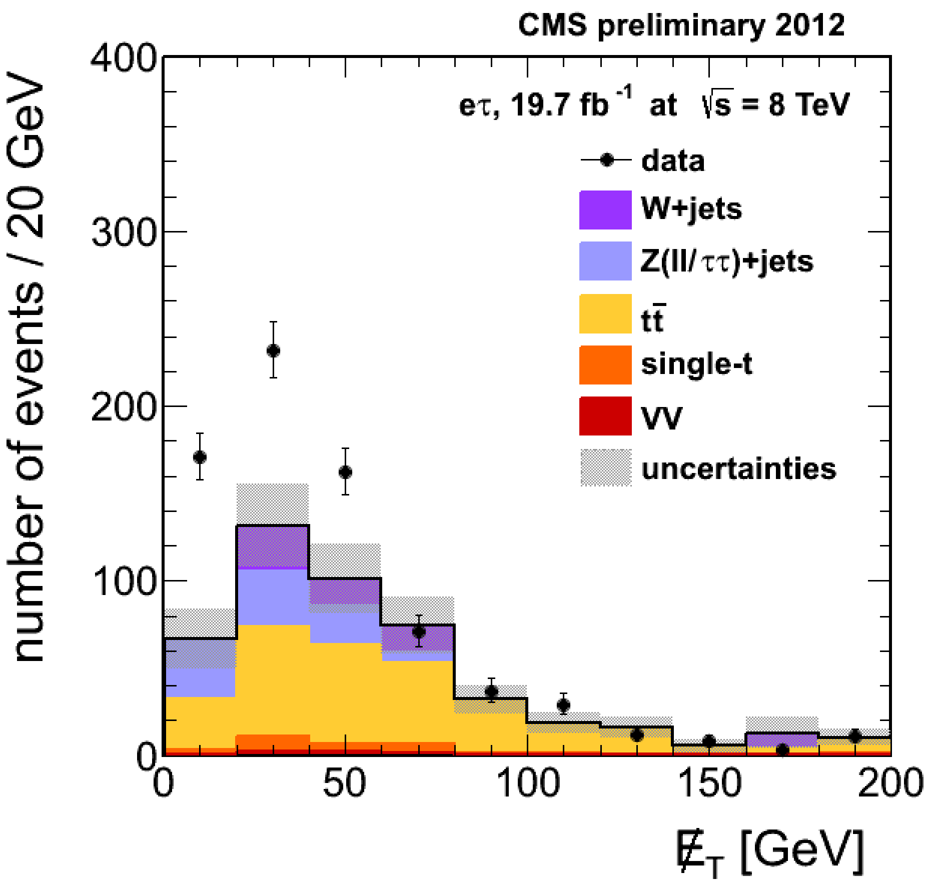

MET in the same-sign control region (used for QCD estimation). The excess at low MET indicates the presence of QCD.

3. Estimate contribution from QCD before the $M(\tau_h,\text{jet})$ cut
4. Extrapolate to final selection by applying efficiency of the $M(\tau_h,\text{jet})$ cut (estimated in same-sign control region with a b-tag veto)
5. Compute S_T distribution by subtracting MC from data in same-sign control region (next slide)

The contribution from QCD (23.6 ± 12.0 events) is added to the major reducible background

QCD Multijets S_T Distribution

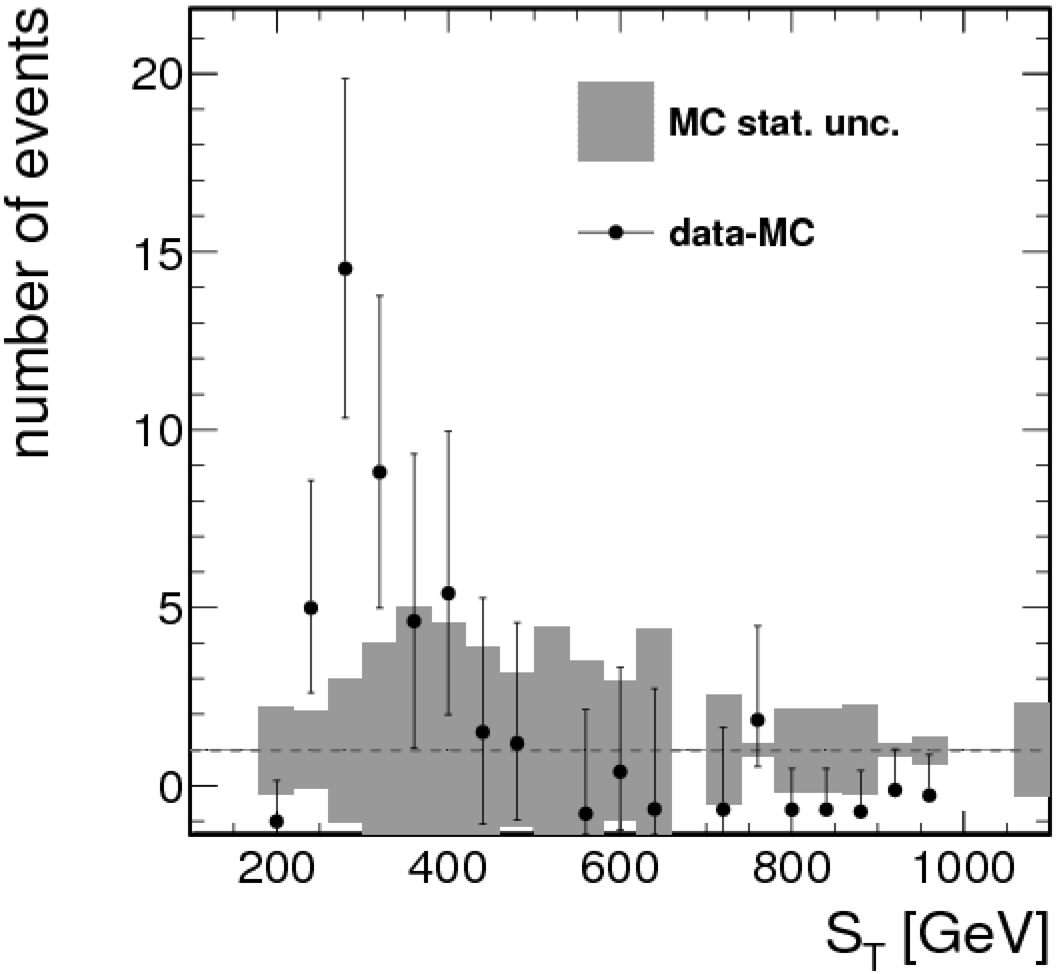

(points lower than 0 are set equal to 0)

Final Selection Cuts

LQ search

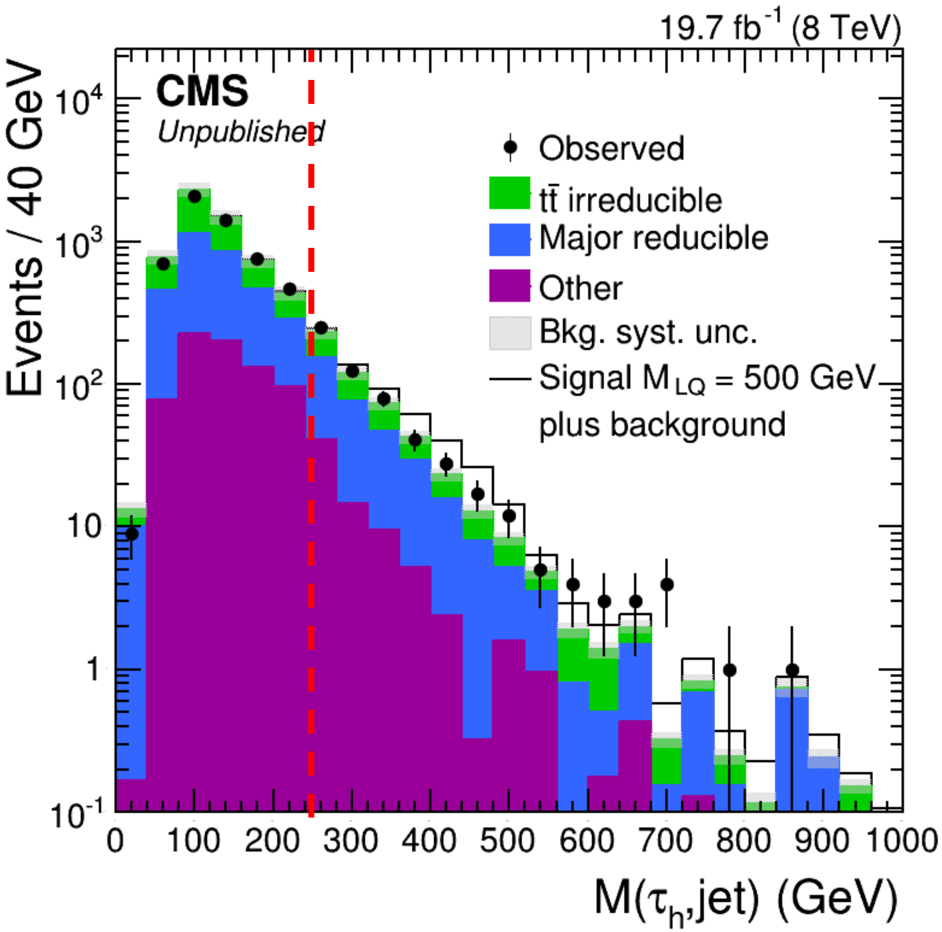

$\tilde{t}$ search

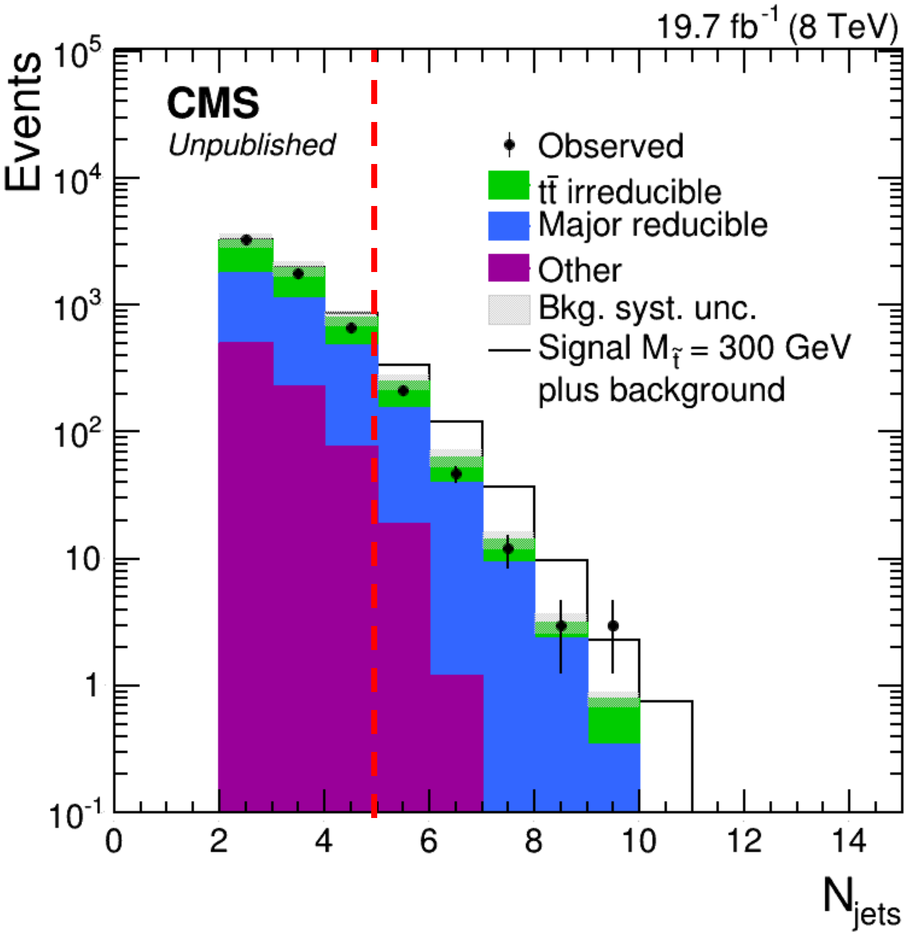

(plots show $e\tau_h$ and $\mu\tau_h$ channels combined, with data-driven background estimations used)

Systematic Uncertainties

Data-driven background uncertainties

Channel		$t\bar{t}$ irreducible	Major reducible
LQ	$e\tau_h$	17%	16%
	$\mu\tau_h$	19%	16%
$\tilde{t}$	$e\tau_h$	16%	24%
	$\mu\tau_h$	17%	23%

Simulated background & signal uncertainties

Source	Uncertainty	Effect on:			
		Signal	Z + jets	Single t	VV
(e, μ) ID, iso, HLT	2%	2%	2%	2%	2%
τ_h ID, iso	6%	6%	6%	6%	6%
b-tagging	~4%	3%	1%	3%	1%
mistagging	~10%	1%	4%	1%	2%
pileup	6%	3%	3%	3%	3%
luminosity	2.6%	2.6%	2.6%	2.6%	2.6%
cross section	–	–	2%	14%	5–15%
statistical	–	–	20–40%	20–40%	20–40%
ISR/FSR	–	4%	–	–	–
τ_h energy scale	3%	0–5%	5–19%	5–19%	5–19%
τ_h energy resolution	10%	1–9%	20%	20%	20%
jet energy scale	~4%	1%	0–7%	0–7%	0–7%
jet energy resolution	5–10%	1%	0–5%	0–5%	0–5%

Also affect S_T distributions

Final Yield Tables

LQ search

	$e\tau_h$	$\mu\tau_h$
$t\bar{t}$ irreducible	105.6 ± 18.1	66.7 ± 12.6
Major reducible	147.8 ± 33.0	117.3 ± 18.9
$Z(\ell\ell/\tau\tau)$ + jets	$21.4 \pm 7.4 \pm 4.9$	$7.5 \pm 4.6 \pm 0.2$
Single t	$16.0 \pm 2.8 \pm 4.4$	$17.3 \pm 2.8 \pm 4.7$
VV	$4.1 \pm 0.6 \pm 1.3$	$2.6 \pm 0.5 \pm 0.8$
Total exp. bkg.	$294.9 \pm 7.9 \pm 39.1$	$211.4 \pm 5.4 \pm 23.4$
Observed	289	216
$M_{LQ} = 500$ GeV	$57.7 \pm 1.4 \pm 5.9$	$51.6 \pm 1.3 \pm 5.3$
$M_{LQ} = 600$ GeV	$20.1 \pm 0.5 \pm 1.9$	$17.7 \pm 0.4 \pm 1.6$
$M_{LQ} = 700$ GeV	$7.1 \pm 0.2 \pm 6.3$	$6.2 \pm 0.1 \pm 5.5$
$M_{LQ} = 800$ GeV	$2.7 \pm 0.1 \pm 0.2$	$2.3 \pm 0.1 \pm 0.2$

$\tilde{t}$ search

	$e\tau_h$	$\mu\tau_h$
$t\bar{t}$ irreducible	88.3 ± 13.7	55.0 ± 9.5
Major reducible	65.7 ± 16.4	59.8 ± 13.8
$Z(\ell\ell/\tau\tau)$ + jets	$4.9 \pm 2.5 \pm 1.1$	$11.6 \pm 5.5 \pm 2.7$
Single t	$3.9 \pm 1.5 \pm 1.1$	$3.5 \pm 1.3 \pm 0.9$
VV	$0.6 \pm 0.2 \pm 0.2$	$0.4 \pm 0.2 \pm 0.1$
Total exp. bkg.	$163.4 \pm 2.9 \pm 21.5$	$130.3 \pm 5.6 \pm 17.1$
Observed	156	123
$M_{\tilde{t}} = 300$ GeV	$94.3 \pm 8.5 \pm 13.2$	$82.8 \pm 8.0 \pm 11.7$
$M_{\tilde{t}} = 400$ GeV	$43.9 \pm 2.6 \pm 4.3$	$38.3 \pm 2.3 \pm 3.8$
$M_{\tilde{t}} = 500$ GeV	$19.4 \pm 0.8 \pm 1.8$	$15.4 \pm 0.7 \pm 1.5$
$M_{\tilde{t}} = 600$ GeV	$6.9 \pm 0.9 \pm 0.7$	$5.7 \pm 0.3 \pm 0.5$

Data-driven estimation uncertainty: ± (syst)

Simulation-based estimation uncertainty: ± (stat) ± (syst)

Final S_T Distributions

LQ search

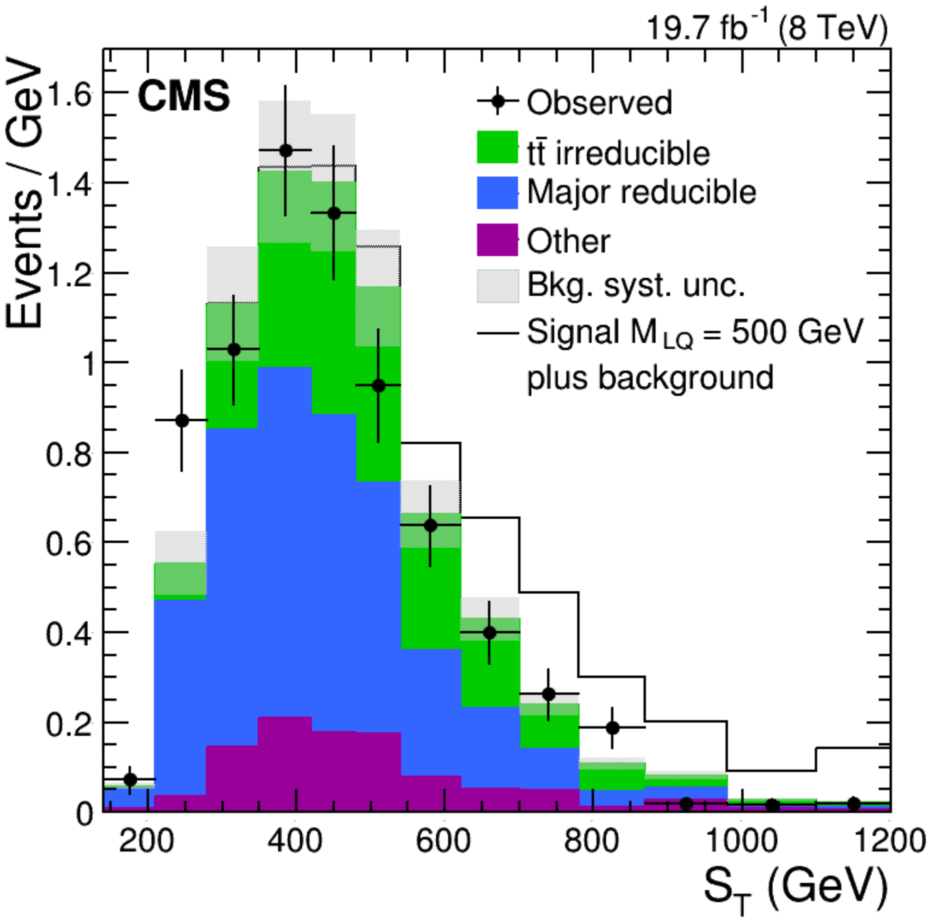

$\tilde{t}$ search

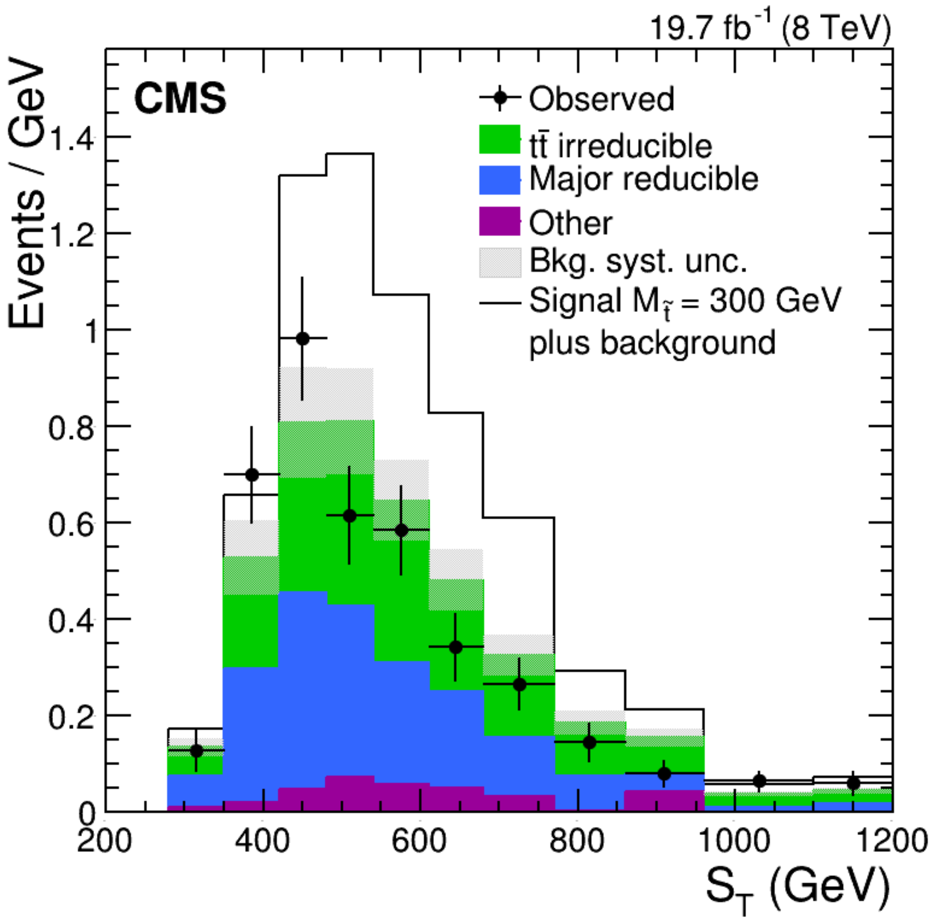

(plots show $e\tau_h$ and $\mu\tau_h$ channels combined)

LQ Search Results

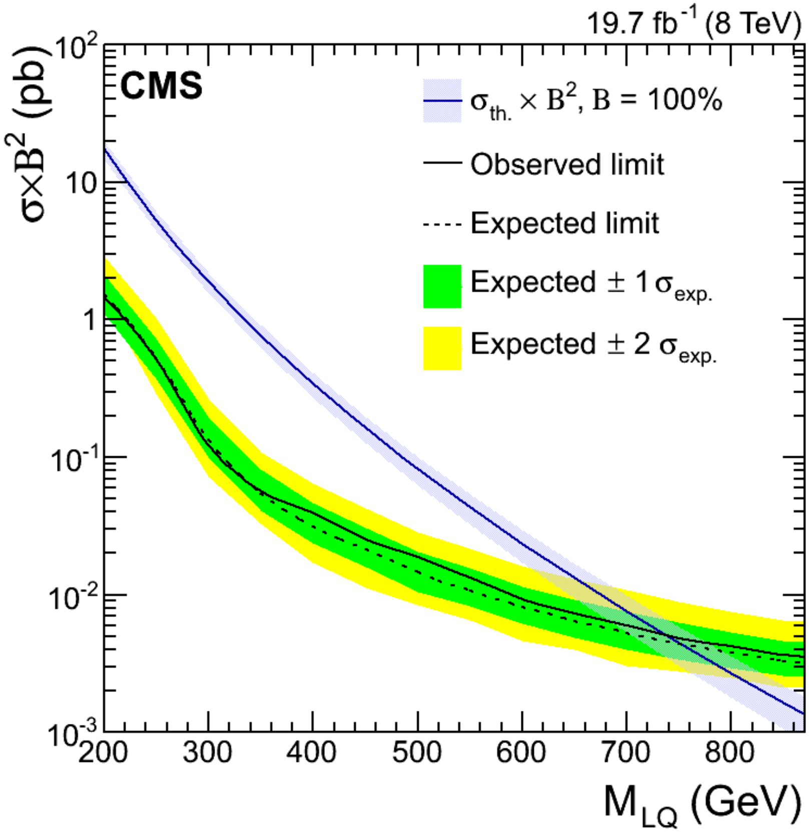

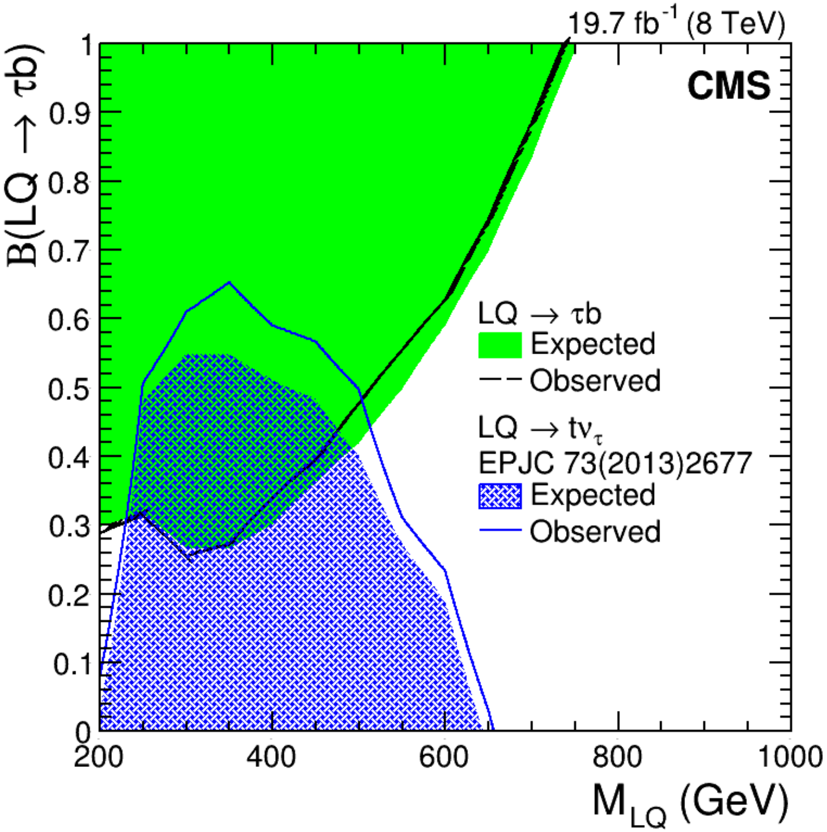

- Assuming $B(LQ_3 \rightarrow b + \tau) = 1$, pair production of third-generation scalar LQs excluded at 95% CL for masses up to **740 GeV** (754 GeV expected)
- Limit applies to top squarks decaying via λ'_{333}
- Previous limit: 530 GeV, from CMS and ATLAS using 7 TeV data
- 95% CL limits also calculated for varying branching fraction (right)

$\tilde{t}$ Search Results

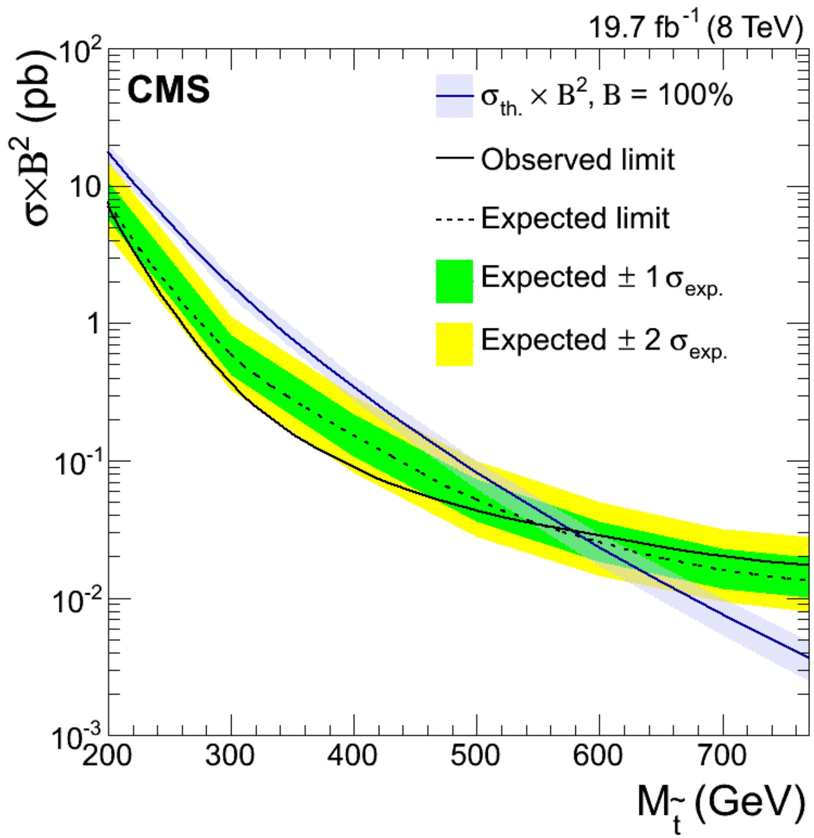

- Assuming 100% branching fraction for the chargino-mediated decay of the top squark involving the λ'_{3jk} coupling, pair production of top squarks excluded at 95% CL for masses up to **576 GeV** (588 GeV expected)
- The first direct search for this decay of the top squark

Leptoquark Prospects

- 2015: Run 2 of the LHC, $\sqrt{(s)}$ = 13 TeV

- Cross section for M_{LQ} = 1000 GeV:
  4.01×10^{-4} pb at $\sqrt{(s)}$ = 8 TeV
  8.36×10^{-3} pb at $\sqrt{(s)}$ = 14 TeV

➢ Possible exclusion of scalar leptoquarks for masses up to 900 – 1200 GeV

➢ Single production of leptoquarks becomes feasible
(limits on λ only extend to TeV scale)

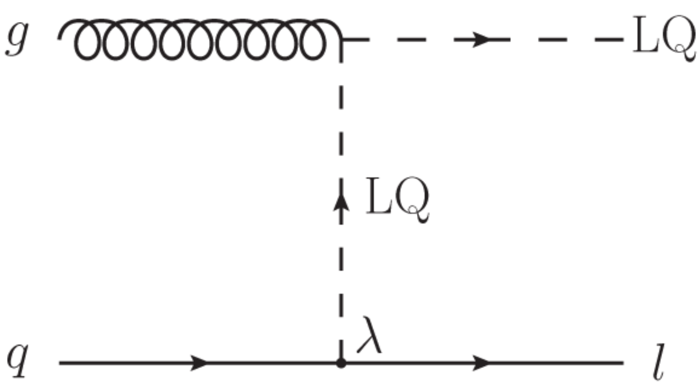

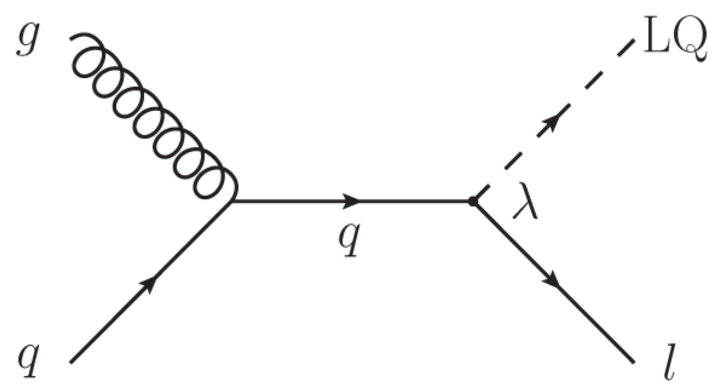

Supersymmetry Prospects

- Similar cross section increases for SUSY particles at √(s) = 13–14 TeV

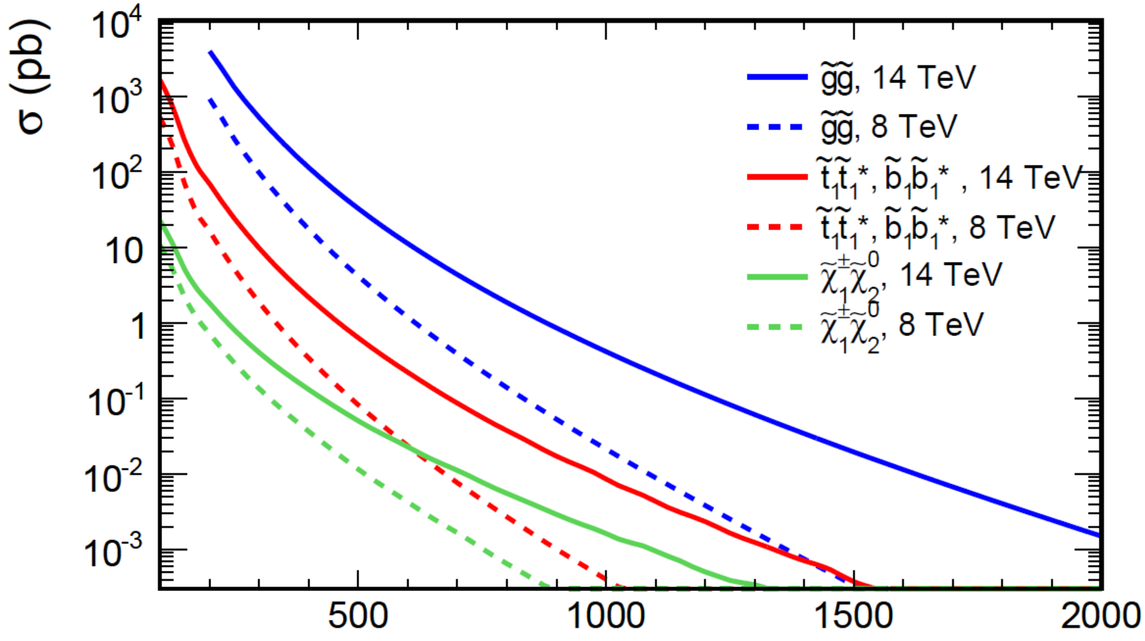

arXiv:1307.7135

- ➢ High discovery potential for gluinos, top squarks, bottom squarks
- ➢ Expand R-parity violating search program to cover more signatures
- ➢ Otherwise, more complete exclusion of natural SUSY

Conclusions

- Search was performed using the full **8 TeV** CMS 2012 dataset, **19.7 fb^{-1}**
- Pair production of third generation scalar leptoquarks has been excluded for masses up to **740 GeV**, assuming B(LQ $\rightarrow$ b + τ) = 1
- These limits apply to top squarks decaying via $\boldsymbol{\lambda'_{333}}$
- Limits for LQ $\rightarrow$ b + τ are also set for varying branching fraction

➢ These limits are the most stringent to date

- Pair production of RPV top squarks with a chargino-mediated decay involving $\boldsymbol{\lambda'_{3jk}}$ has been excluded for masses up to **576 GeV**, assuming a branching fraction of 100%

➢ This is the first direct search for top squarks decaying to such a final state

- Published in *Phys. Lett. B* 739 (2014) 229 (arXiv:1408.0806, twiki)

Backup

The Standard Model

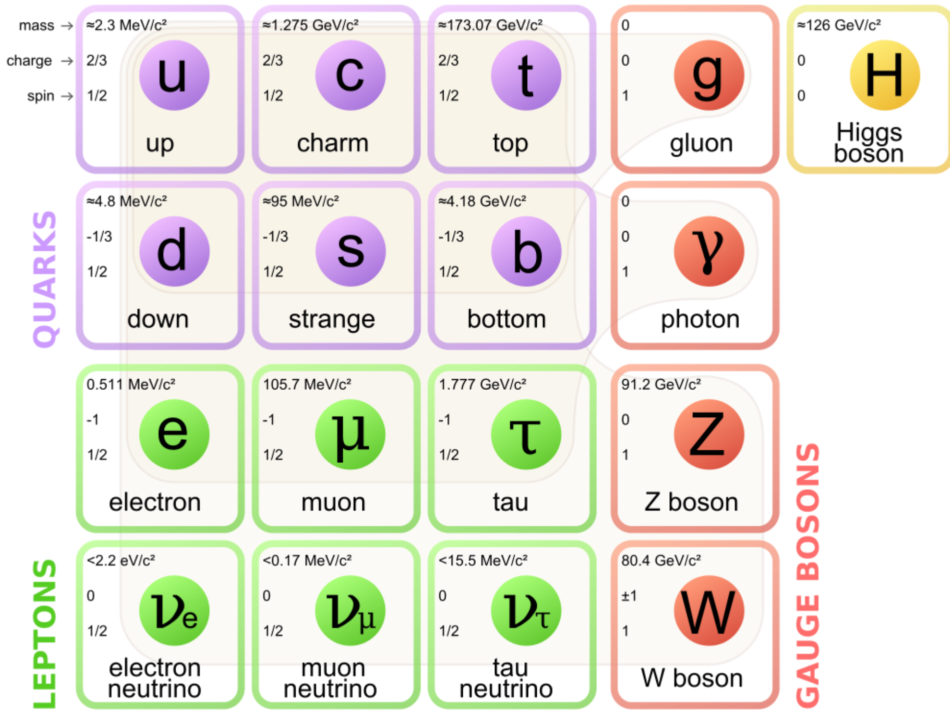

(source)

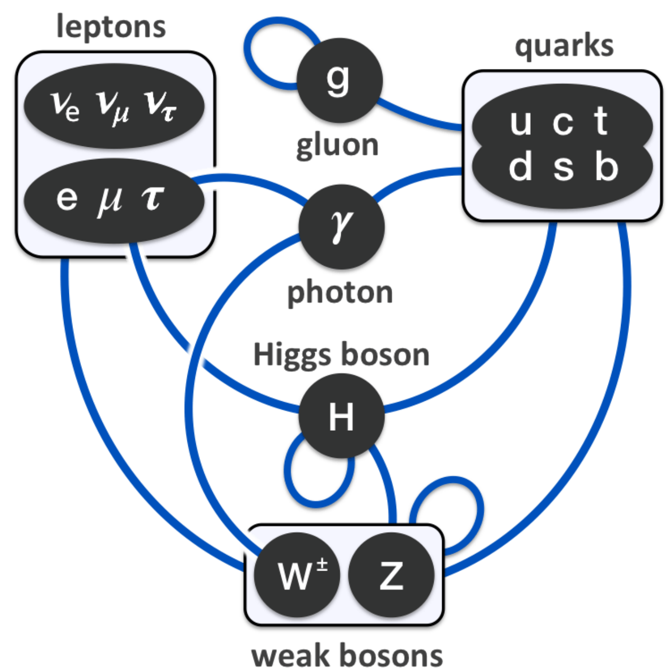

(source)

- Three generations of matter
- Three fundamental forces: electromagnetism, weak, strong
- Higgs mechanism for electroweak symmetry breaking and fermion masses
- Confirmed by decades of precise experimental tests

The Large Hadron Collider

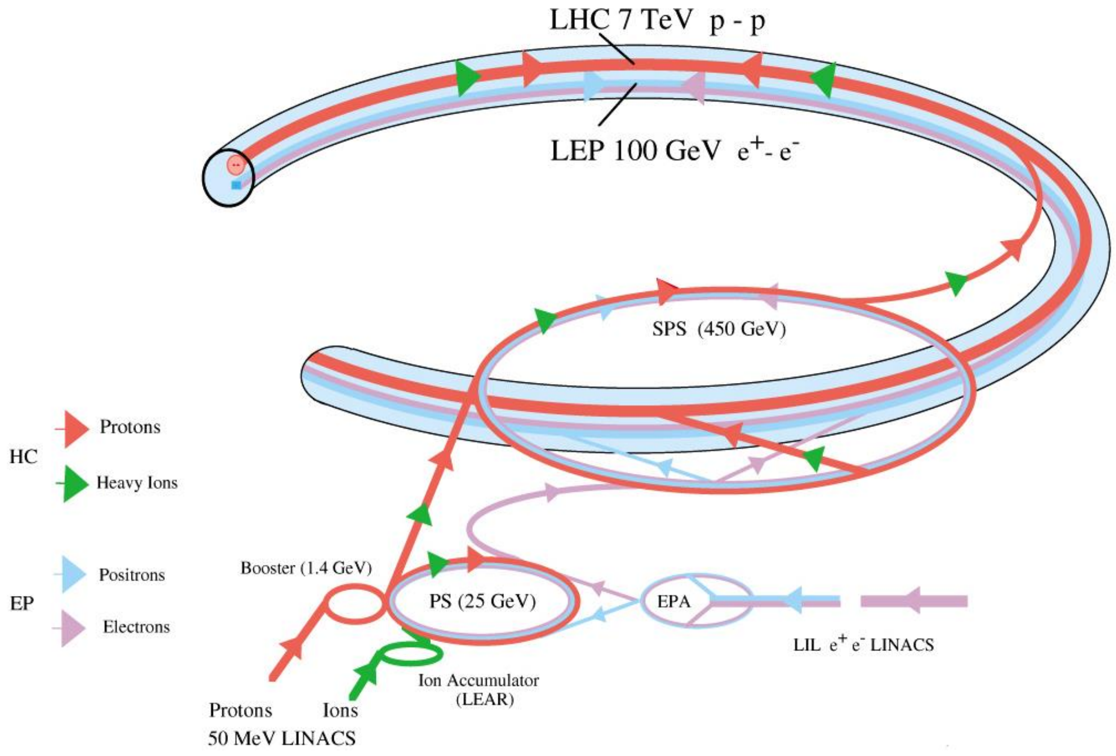

- Circumference of 26.7 km
- 1232 dipole magnets, NbTi superconductors cooled to 1.9 K
- Design parameters: $\sqrt{(s)}$ = 14 TeV, $\mathcal{L} = 10^{34}$ cm^{-2} s^{-1}, 25 ns bunch spacing
- 2012 run: $\sqrt{(s)}$ = 8 TeV, $\mathcal{L} = 7.67\times10^{33}$ cm^{-2} s^{-1} (peak), 50 ns bunch spacing

Tracker

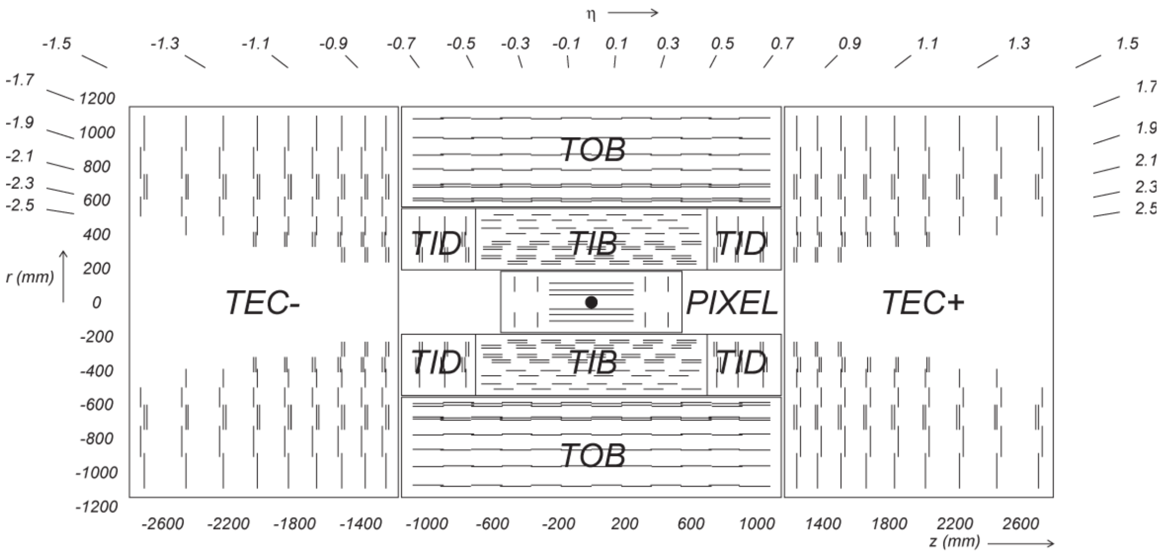

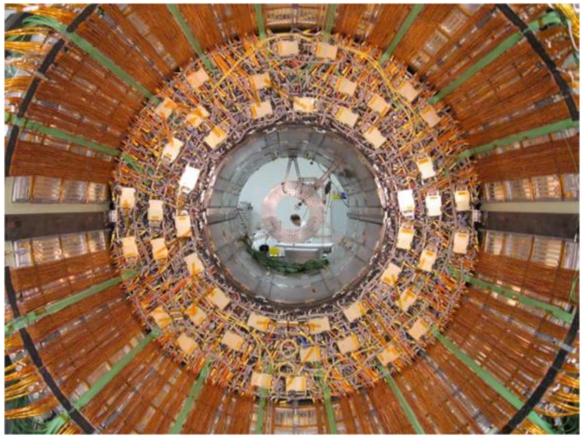

Tracker Outer Barrel

- Pixel: hybrid silicon detector, resolution 10 μm × 20 μm (r × z)
  - BPIX: Barrel Pixel, 3 layers, 48 million pixels
  - FPIX: Forward Pixel, 2 layers, 18 million pixels
- Silicon Strip Detector:
  - Tracker Inner Barrel (TIB), Tracker Inner Disks (TID), Tracker Outer Barrel (TOB), Tracker EndCaps (TEC) → 9.3 million total strips
- Charged particles create tracks

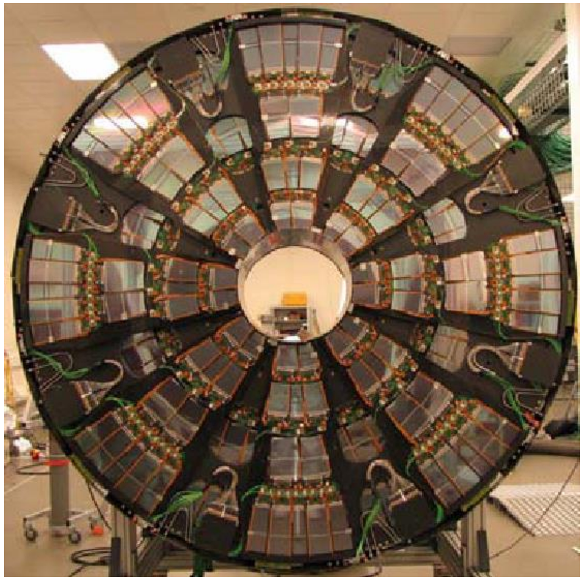

Tracker EndCap

Electromagnetic Calorimeter (ECAL)

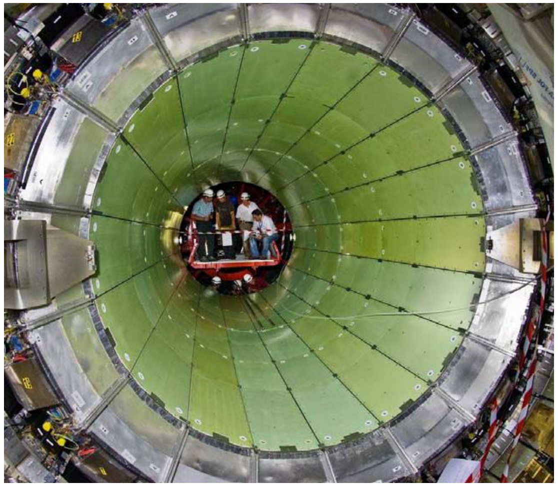

ECAL Barrel

ECAL Endcap

- $PbWO_4$ crystals have short radiation length (0.89 cm) and small Molière radius (2.2 cm)
- ECAL Barrel (EB, $0 < |\eta| < 1.479$): $PbWO_4$ crystals, avalanche photodiodes
- ECAL Endcap (EE, $1.479 < |\eta| < 3.0$): $PbWO_4$ crystals, vacuum phototriodes
- Preshower (ES, $1.653 < |\eta| < 2.6$): Lead absorber, silicon sensor, 2 layers
- Measures photons and charged particles

Hadron Calorimeter (HCAL)

- HCAL Barrel (HB, $0 < |\eta| < 1.3$):
  Brass absorber, plastic scintillator, HPDs
  16+1 layers

- HCAL Endcap (HE, $1.3 < |\eta| < 3.0$):
  Brass absorber, plastic scintillator, HPDs
  16+1 layers

- HCAL Outer (HO, $0 < |\eta| < 1.3$):
  Brass absorber, plastic scintillator, HPDs
  1+1 layers

- HCAL Forward (HF, $3.0 < |\eta| < 5.0$):
  Steel absorber, quartz fibers, PMTs

- Measures charged and neutral hadrons

HCAL Barrel

HCAL Endcap

Superconducting Solenoid

Solenoid mounted vertically, before installation

Artistic rendering

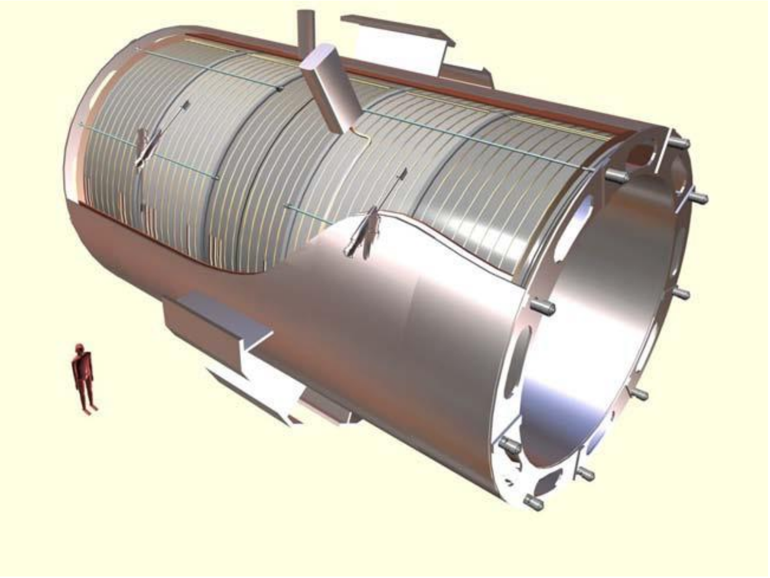

- NbTi conductor, cooled to 4.5 K
- Magnetic field of 3.8 T
- Stored energy of 2.35 GJ

Muon System

- Drift Tubes (DTs): Muon Barrel (MB)
  85% Ar, 15% CO_2; drift time 400 ns
- Cathode Strip Chambers (CSCs): Muon Endcap (ME)
  40% Ar, 50% CO_2, 10% CF_4; drift time 60 ns
- Resistive Plate Chambers (RPCs): MB & ME
  96.2% $C_2H_2F_4$, 3.5% iC_4H_{10}, and 0.3% SF_6
  Drift time < 3 ns: fast, used for triggering

Compare to 50 ns bunch crossing

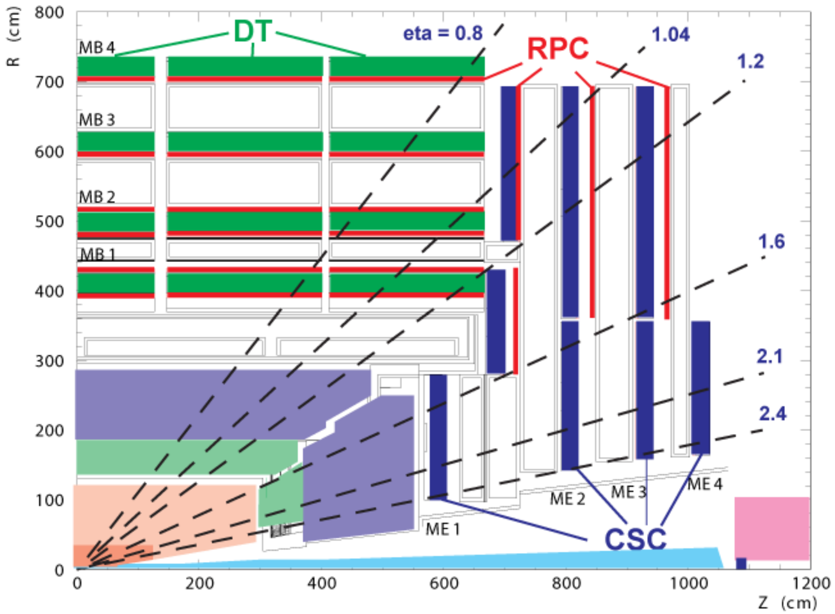

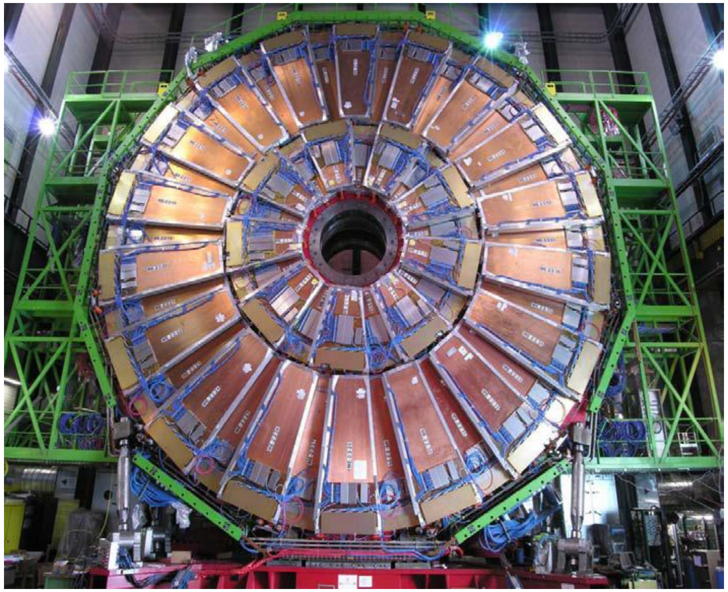

CSCs (Muon Endcap)

Trigger

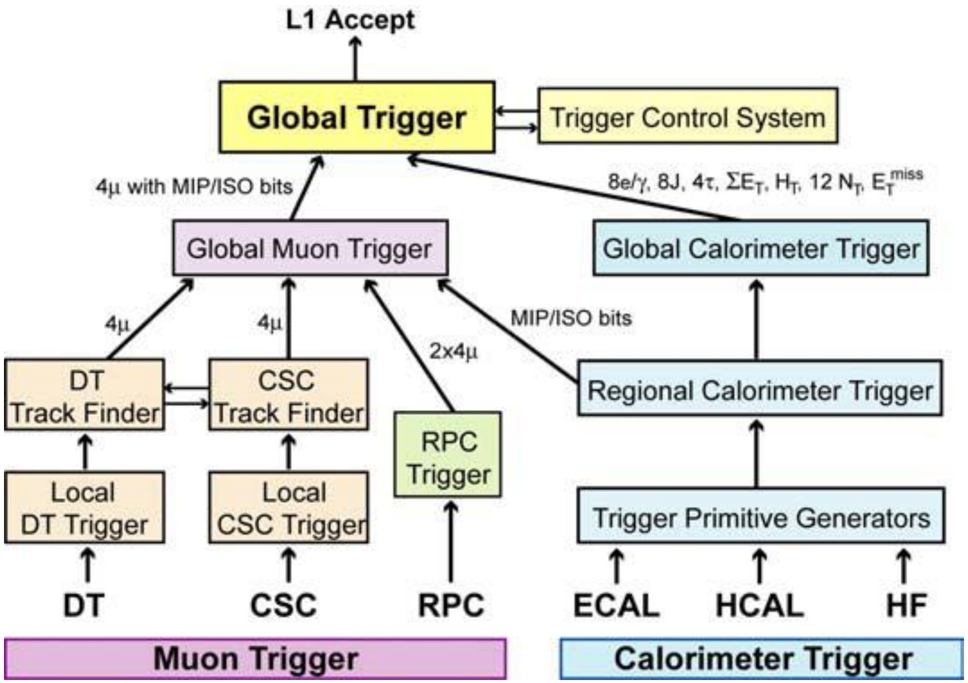

- LHC produces 20 million collision events per second
- At ~1 MB per event, this becomes 20 TB per second
- Far too much data to process and store
- Plus, most events are not interesting

- Level 1 (L1): 3.2 μs/event, 100 kHz rate → selects 1 out of 200 events
- High Level Trigger (HLT): 200 ms/event, O(100 Hz) rate → selects 1 out of 1000 L1 events
- In total, keep only 1 out of 200,000 events → 100 MB per second (~100 petabytes over the course of the 2012 run)

Electrons

- Electrons lose energy via bremsstrahlung as they traverse the tracker → track curvature increases with radial distance in the tracker
- Gaussian Sum Filter (GSF):
  use a mixture of Gaussians to select the electron track
  match to ECAL clusters (or superclusters)
- Various requirements for shower shape variables, energy variables, relative Particle Flow isolation (w/ area-based pileup correction)

Muons

- Match trajectories and momenta of charged-particle tracks with muon tracks
- Various requirements for tracker hits, muon system hits, global track fit, relative Particle Flow isolation (w/ $\Delta\beta$ pileup correction)

Jets

- Particle Flow candidates clustered together using anti-k_t algorithm, R = 0.5
- 65% charged (tracker), 25% photons (ECAL), 10% neutral hadrons (HCAL)
- Offset correction from minimum bias, relative (η) correction from dijets, absolute (p_T) correction from γ/Z + jets

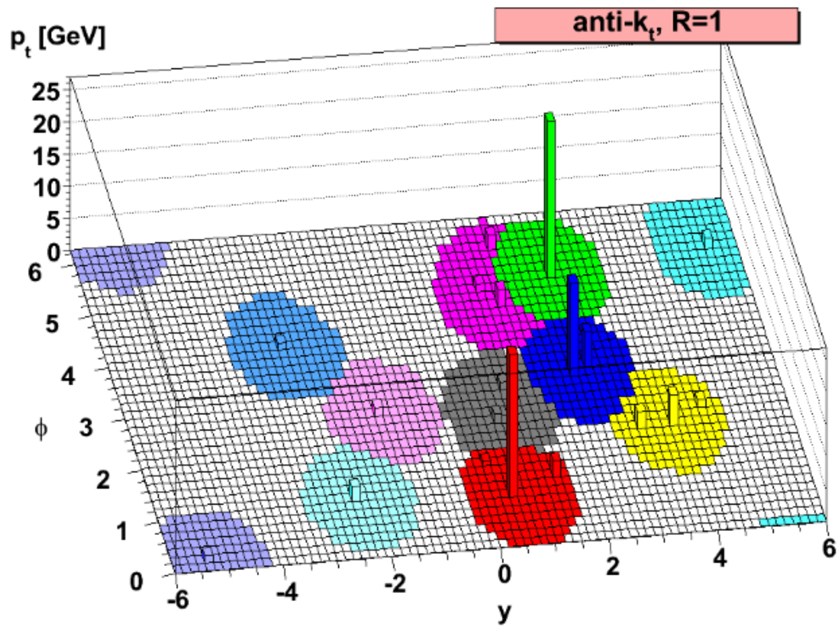

arXiv:0802.1189

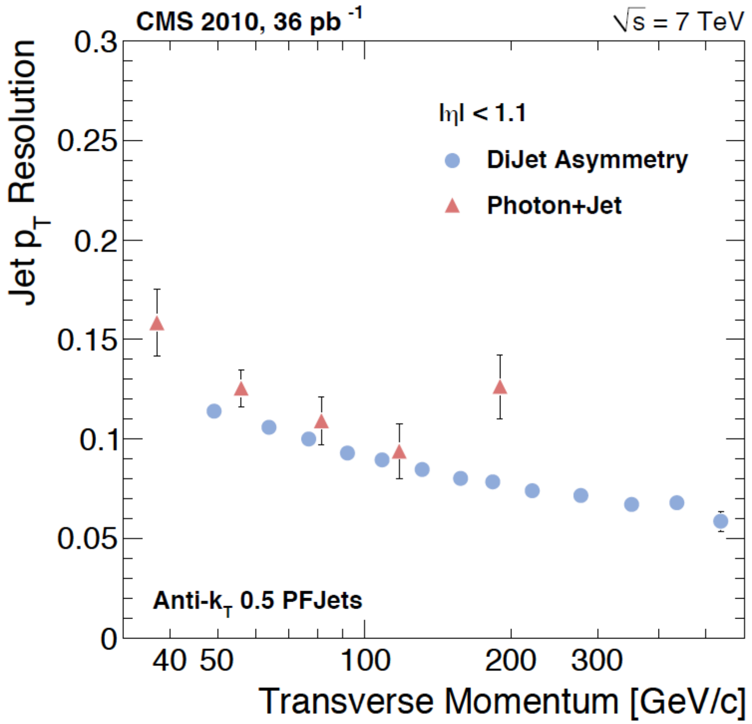

arXiv:1107.4277

b-tagging

- Combined Secondary Vertex (CSV) algorithm
- Use the adaptive vertex fitter to identify vertices near the jet and far from the primary vertex
- Combine these vertices with high-quality tracks from the jet
- Calculate a likelihood-based discriminator

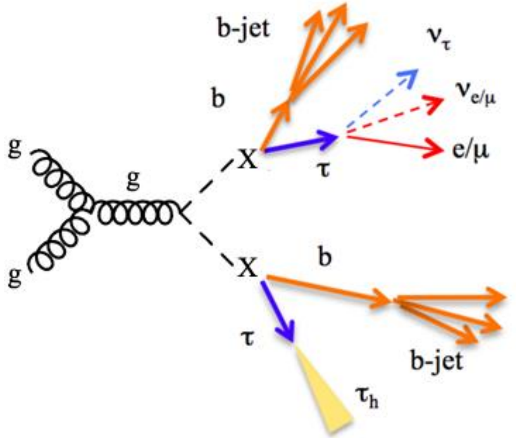

Figure 11 from Angela Barbaro Galtieri et al 2012 Rep. Prog. Phys. 75 056201

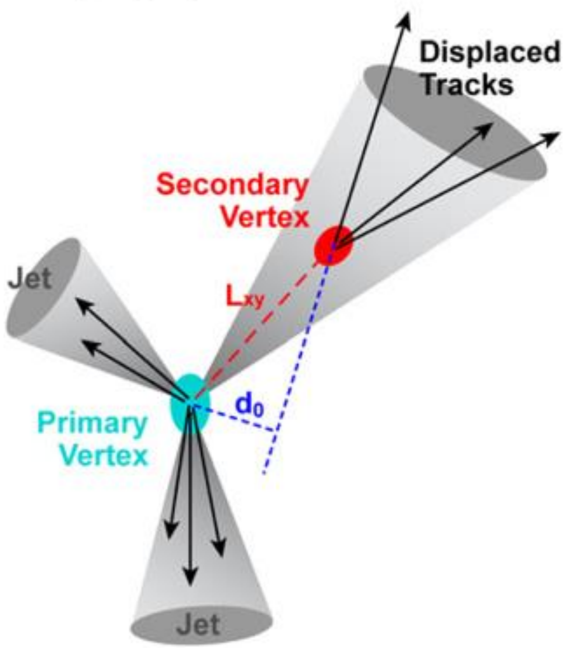

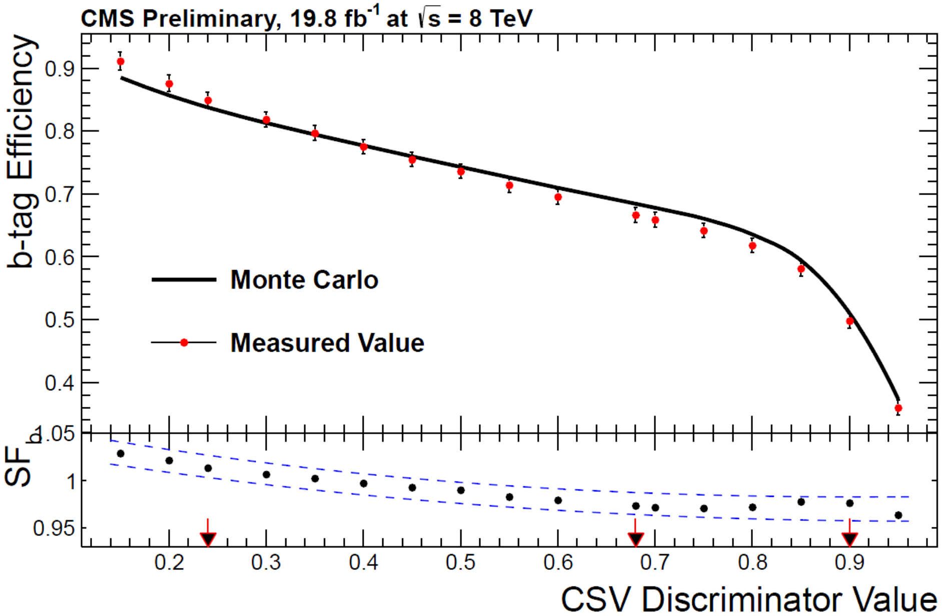

CMS-PAS-BTV-13-001

Object Identification (Full)

Muon

$p_T > 30$ GeV, $|\eta| < 2.1$
Tight ID, relative isolation
Vertex quality check

Electron

$p_T > 30$ GeV, $|\eta|$ in ECAL fiducial
Medium ID, relative isolation
Vertex quality check

Tau

$p_T > 30$ GeV, $|\eta| < 2.3$
Decay mode finding (HPS)
Loose combined isolation (3 hits)
Discriminators:
e-τ loose MVA3, μ-τ tight/loose v2

Jets

$p_T > 30$ GeV, $|\eta| < 2.4$
Loose PF Jet ID
b-tagging: loose, CSV > 0.244

HLT

HLT_IsoMu24
HLT_Ele27_WP80

Corrections

Pileup reweighting
Lepton data/MC efficiency
b-tag & mistag scale factors

Object ID Working Points

Muon ID

Working Point	
Tight	Loose
PF muon	PF muon
Global muon	Global muon OR tracker muon
$I_\mu^{\mathrm{PF}}/p_{\mathrm{T}} < 0.12$	$I_\mu^{\mathrm{PF}}/p_{\mathrm{T}} < 0.3$
$d_0 < 0.2\,\mathrm{cm}$	
$d_z < 0.5\,\mathrm{cm}$	
Global track fit $\chi^2/n_{\mathrm{dof}} < 10$	
Global track fit $n_{\mathrm{muon\ segment}} > 0$	
$n_{\mathrm{hits}}(\mathrm{pixel}) > 0$	
$n_{\mathrm{layers}}(\mathrm{tracker}) > 5$	
$n_{\mathrm{stations}}(\mathrm{muon}) > 1$	

Electron ID

Cut Variable	Cut Value			
	Medium		Loose	
	Barrel	Endcap	Barrel	Endcap
$I_{\mathrm{e}}^{\mathrm{PF}}/p_{\mathrm{T}} <$	0.15	0.15	0.15	0.15
$\sigma_{i\eta i\eta} <$	0.01	0.03	0.01	0.03
$\lvert\Delta\phi_{\mathrm{in}}\rvert <$	0.06	0.03	0.15	0.10
$\lvert\Delta\eta_{\mathrm{in}}\rvert <$	0.004	0.007	0.007	0.009
$H/E <$	0.12	0.10	0.12	0.10
$\lvert d_0^{\mathrm{vtx}}\rvert <$	0.02	0.02	0.02	0.02
$\lvert d_z^{\mathrm{vtx}}\rvert <$	0.1	0.1	0.2	0.2
$\lvert 1/E - 1/p\rvert <$	0.05	0.05	0.05	0.05

Jet ID

Cut Variable	Cut Value
	Loose
$f_{\mathrm{CH}} >$	0.0
$f_{\mathrm{NH}} <$	0.99
$f_\gamma <$	0.99
$f_{\mathrm{EM}} <$	0.99
$n_{\mathrm{charged}} >$	0
$n_{\mathrm{constituents}} >$	1

CL_s Limits from S_T Distribution

- Null hypothesis H_0: b, background-only
  Signal hypothesis H_1: s + b, signal + background
- $P(\theta; N_H)$: Poisson probability to observe θ events in data given the hypothesis H which predicts N_H events, accounting for nuisance parameters
- Define the test statistic Q using the binned S_T distribution, split into $e\tau_h$ and $\mu\tau_h$ channels:

$$\mathcal{Q} = \prod_{i=e\tau_{\mathrm{h}},\,\mu\tau_{\mathrm{h}}} \prod_{j=0}^{n_{\mathrm{bin}}} \frac{\mathcal{P}_{i,j}(\theta; N_{H_1})}{\mathcal{P}_{i,j}(\theta; N_{H_0})}$$

- Perform numerous pseudo-experiments, varying θ, to compute a distribution of Q values for each hypothesis; compute Q with $\theta = N_{obs}$ to get Q_{obs}
- Calculate CL_s as follows:

$$\mathrm{CL}_{s+b} = \mathcal{P}(\mathcal{Q}_{H_1} \leq \mathcal{Q}_{\mathrm{obs}})$$
$$\mathrm{CL}_{b} = \mathcal{P}(\mathcal{Q}_{H_0} \leq \mathcal{Q}_{\mathrm{obs}})$$
$$\mathrm{CL}_{s} = \mathrm{CL}_{s+b}/\mathrm{CL}_{b}$$

- Repeat the calculation of CL_s for different signal mass hypotheses
- Masses with $CL_s \leq 1 - \alpha$ are excluded at the α confidence level (95%)

Lepton p_T (preselection)

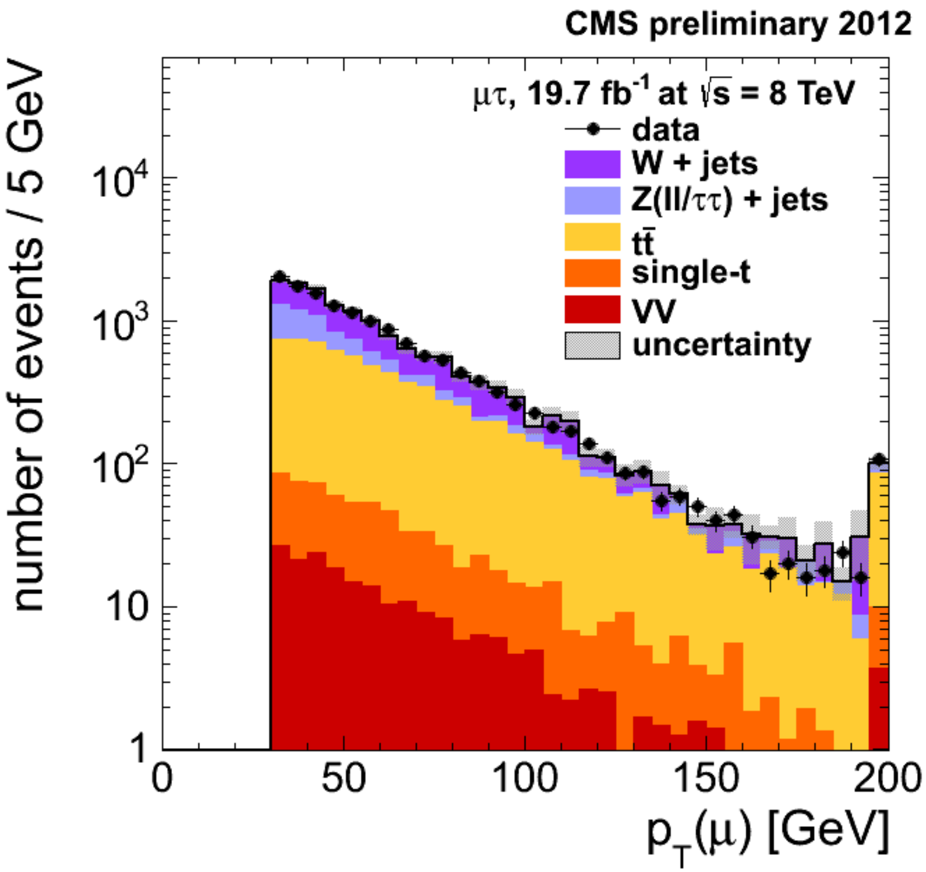

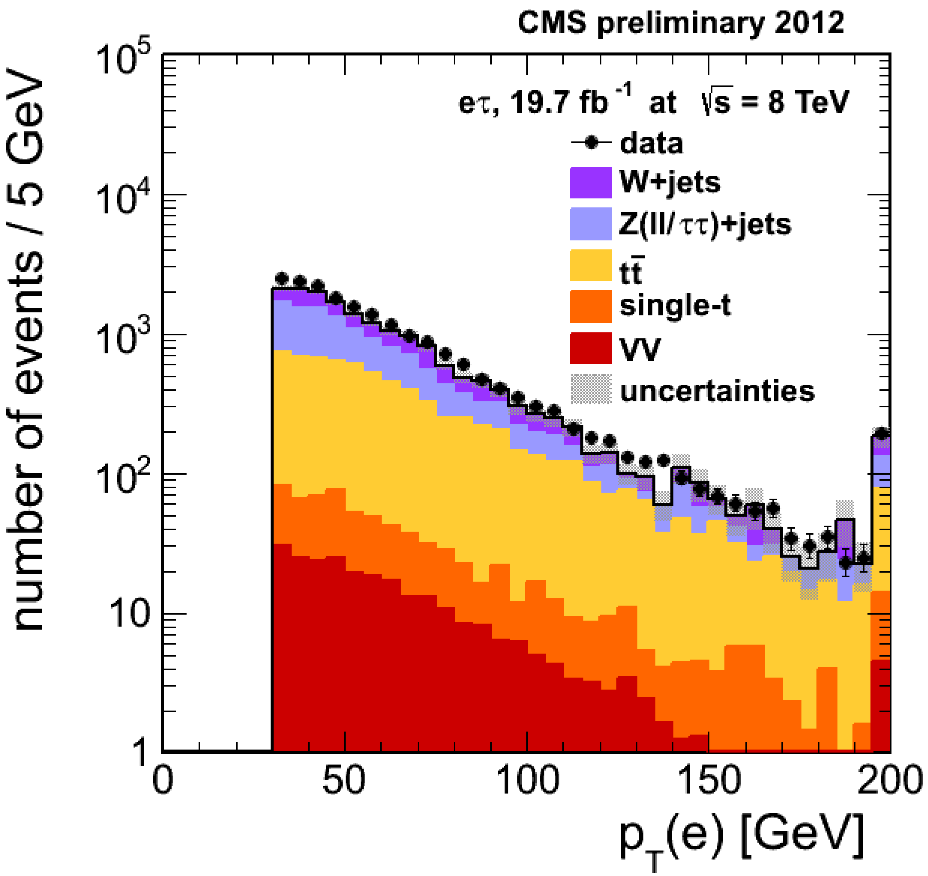

Good data/MC agreement for both channels

Tau p_T (preselection)

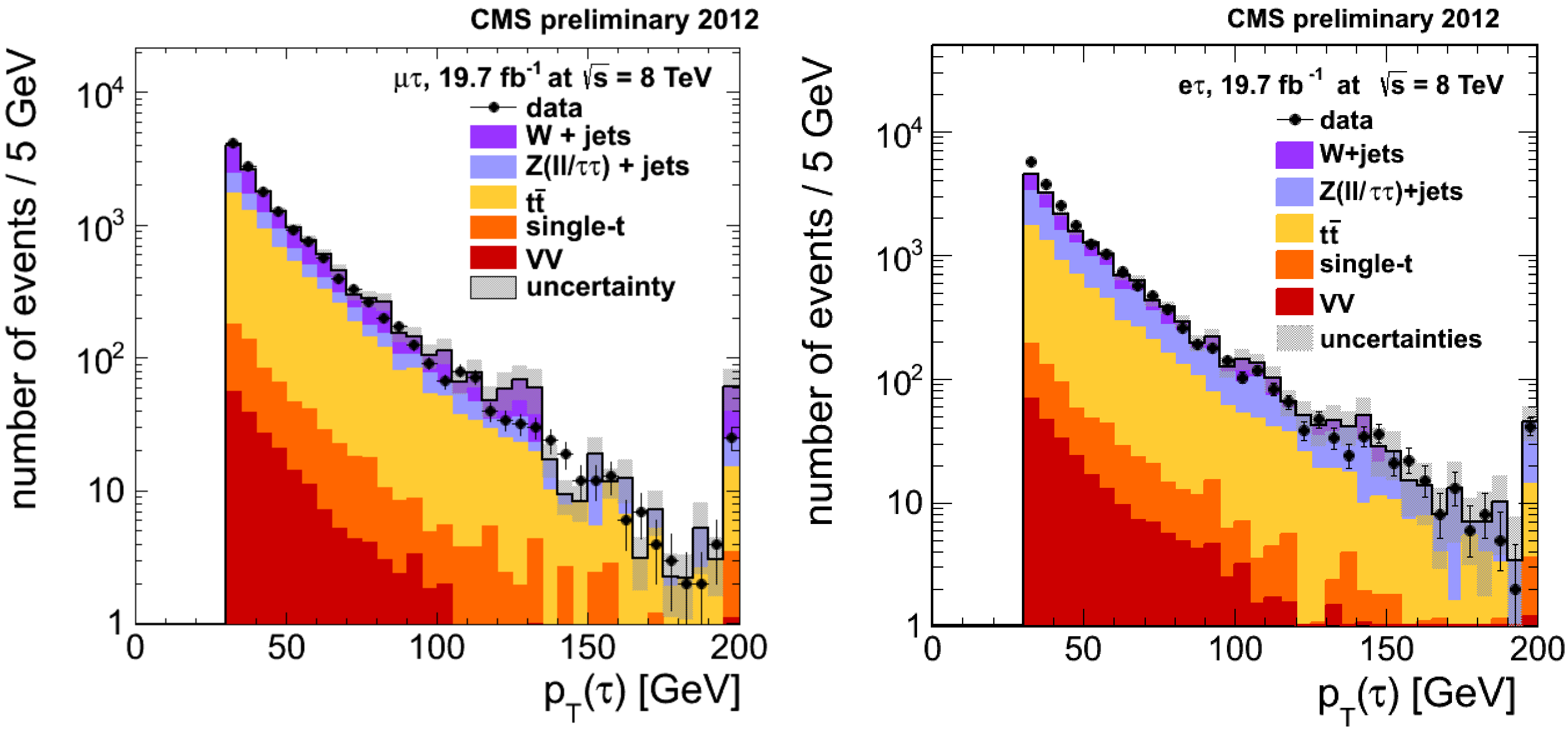

Good data/MC agreement for both channels

b-jet Multiplicity (preselection)

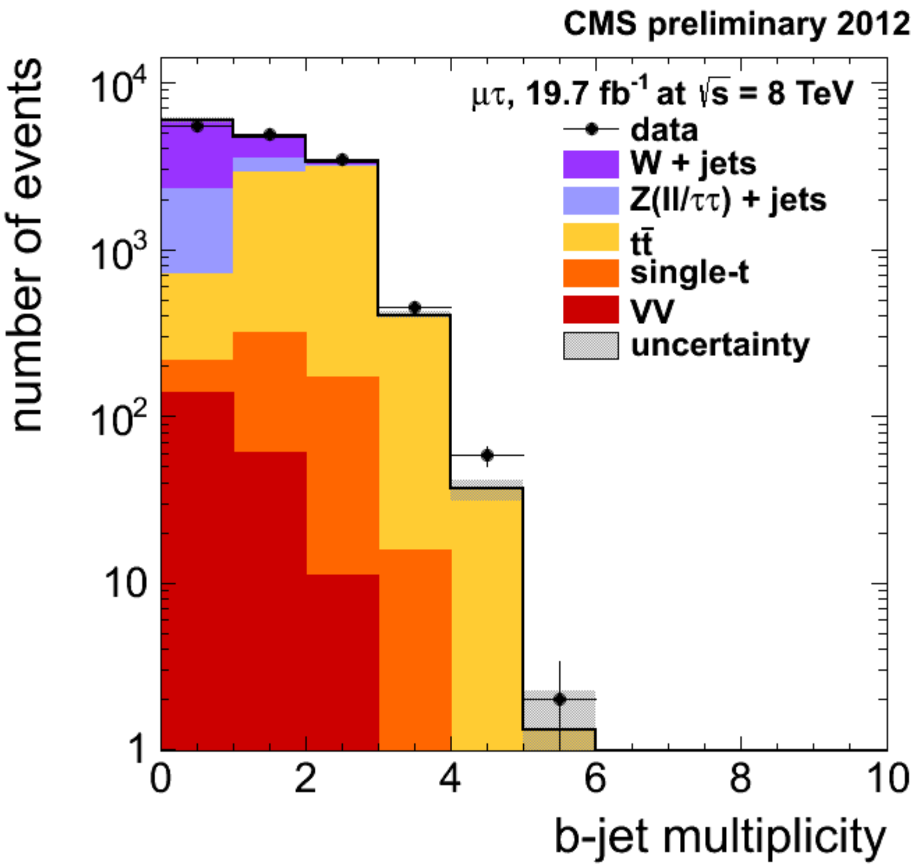

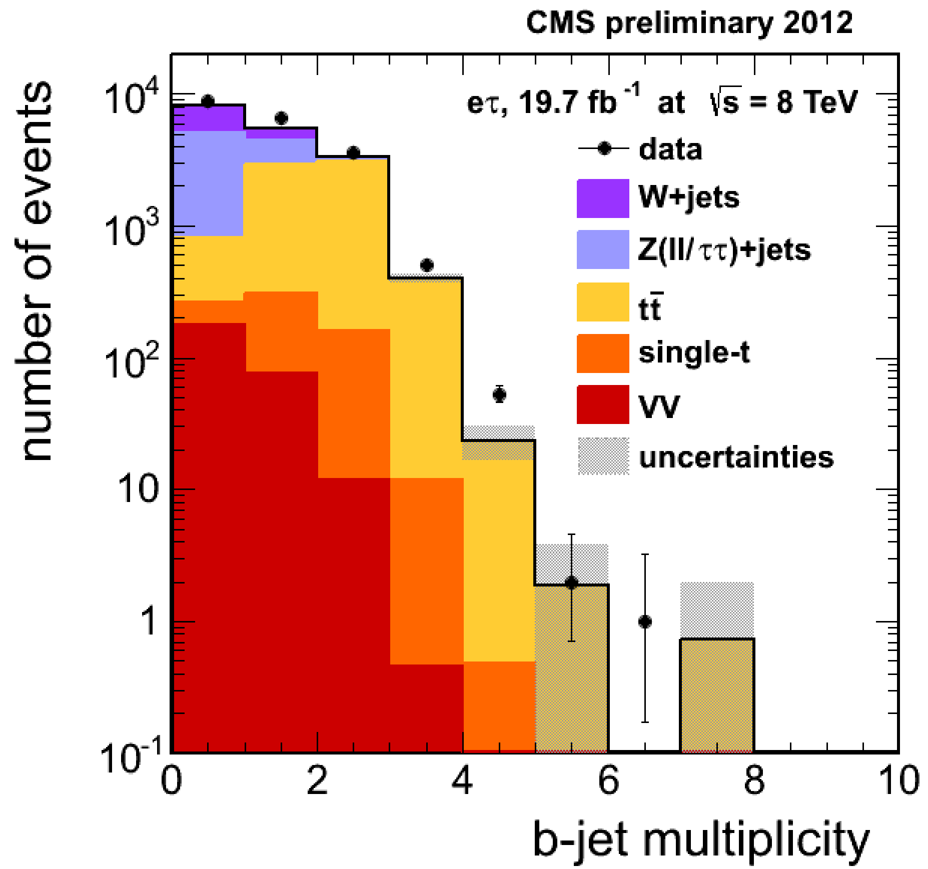

Good data/MC agreement for both channels

Mass of $\ell + \tau$ (preselection)

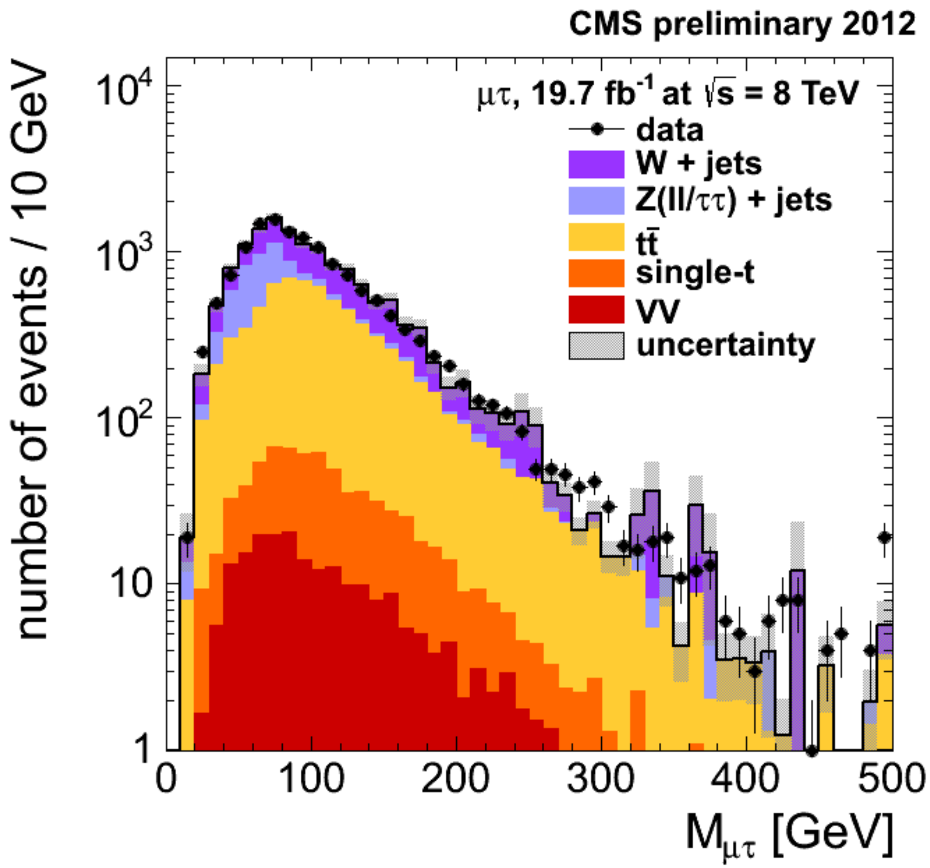

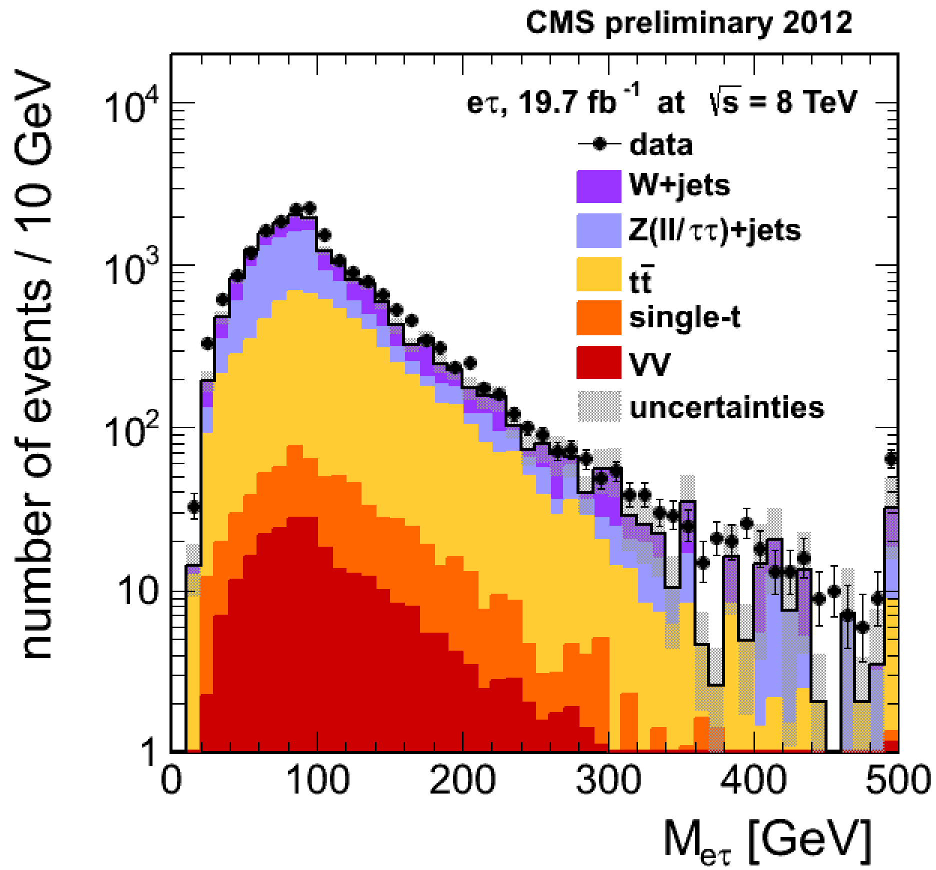

Good data/MC agreement for both channels

Lepton η (preselection)

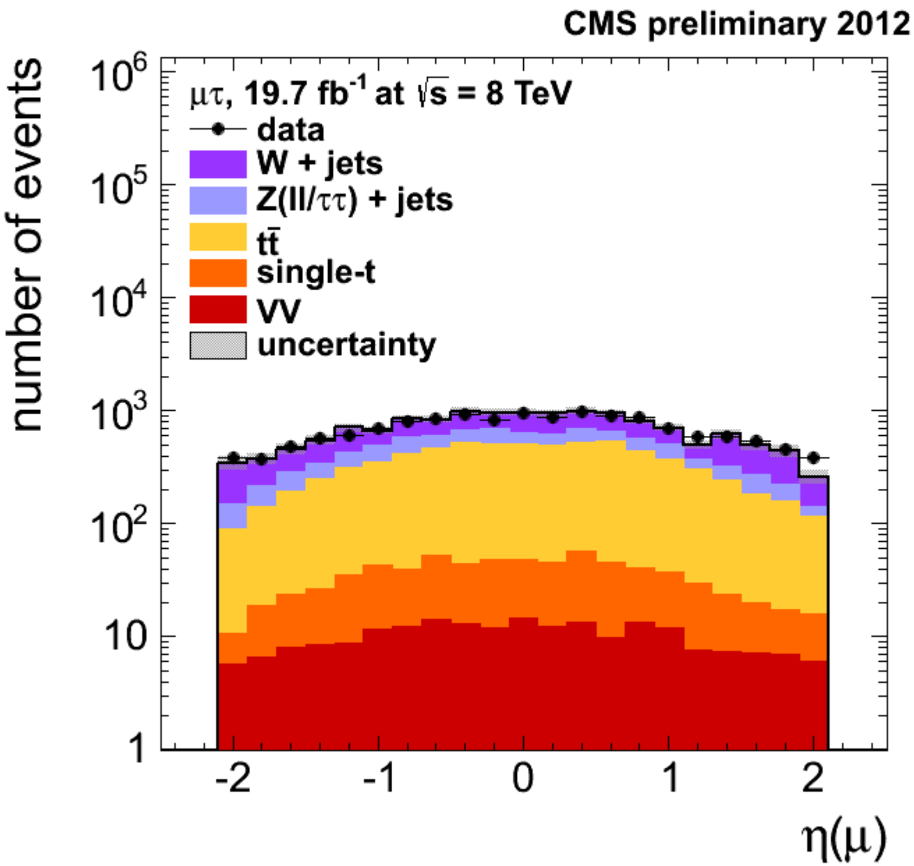

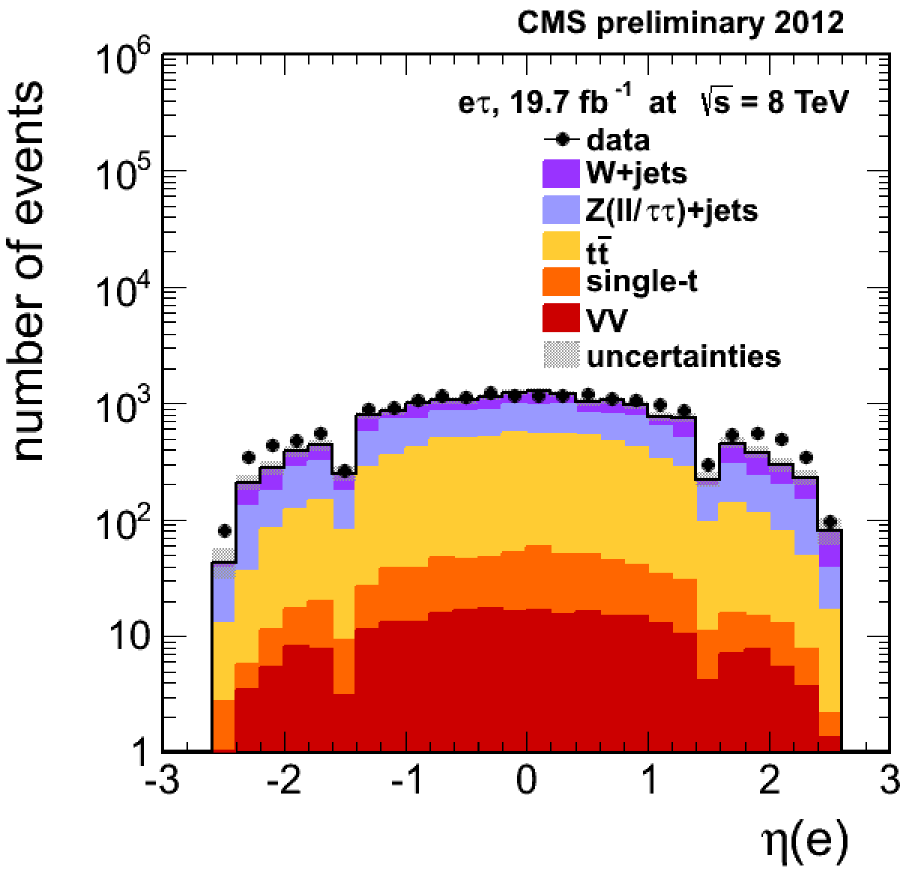

Good data/MC agreement for both channels

Tau η (preselection)

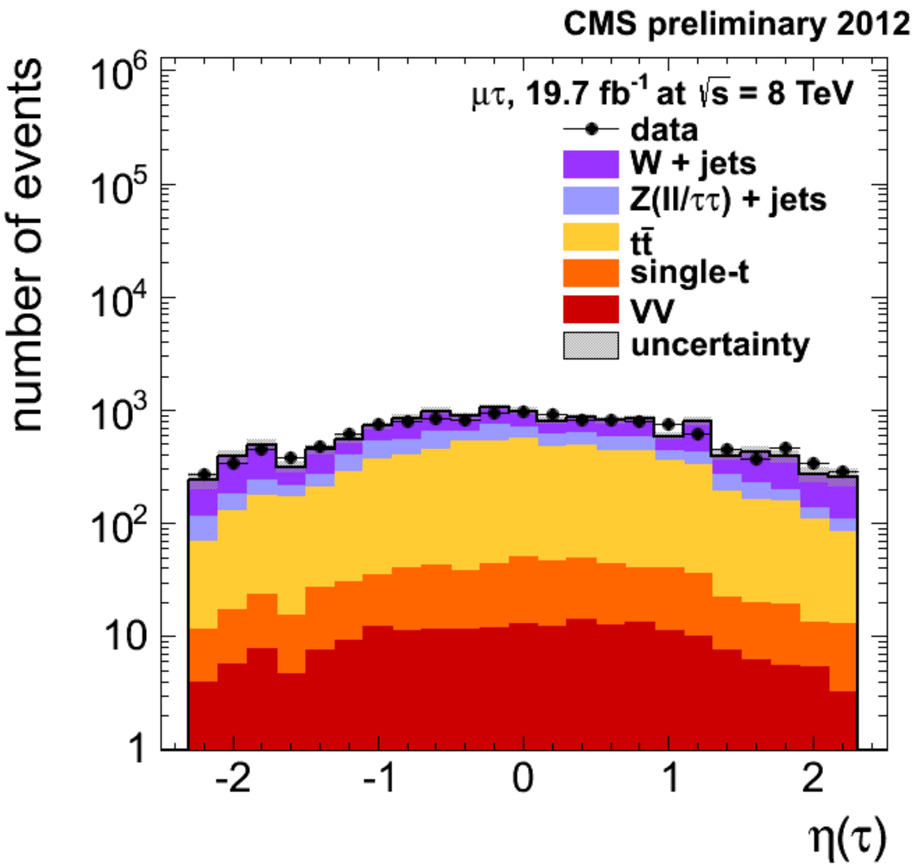

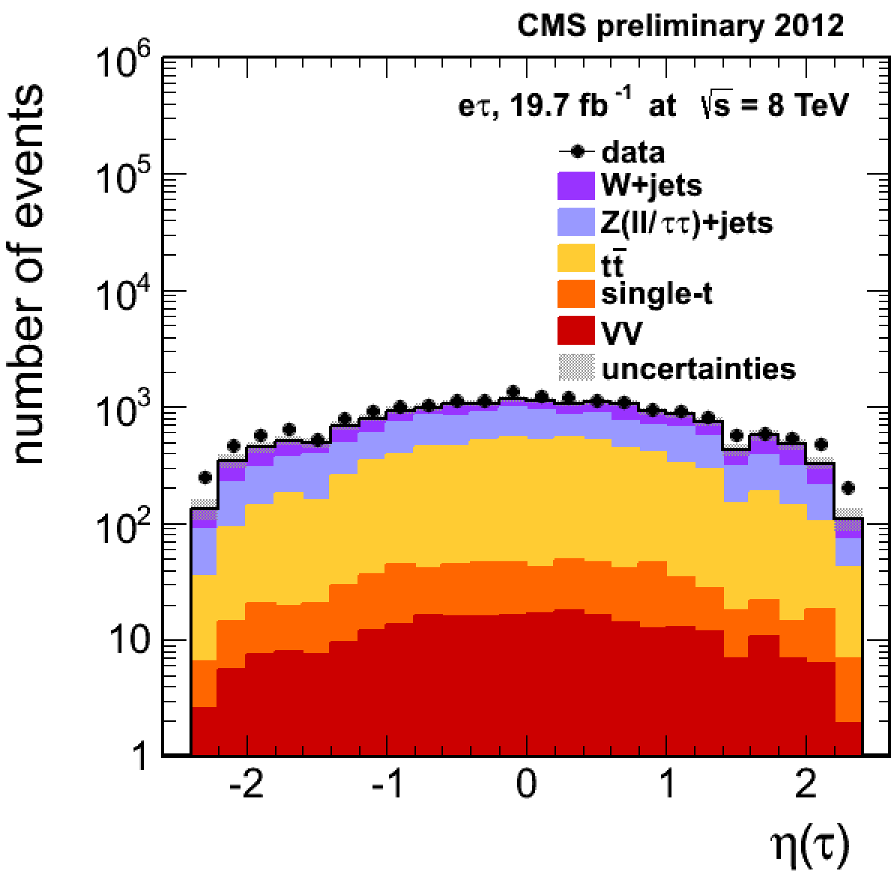

Good data/MC agreement for both channels

Preselection Yields

	$e\tau_h$ channel	$\mu\tau_h$ channel
W + jets	4221.6 ± 188.1	4846.3 ± 233.6
Z + jets	4766.7 ± 85.1	2369.1 ± 80.7
$t\bar{t}$	6272.2 ± 65.5	6430.5 ± 69.8
Single t	462.9 ± 14.4	512.3 ± 16.0
VV	223.4 ± 4.4	212.5 ± 4.6
QCD multijets	(2452.6 ± 512.1)	—
Total Bkg. (no QCD)	15946.8 ± 232.9	14370.8 ± 257.3
Data	18177	14351